

# Mild-split SUSY with flavor

Latif Eliaz, Amit Giveon, Sven Bjarke Gudnason and Eitan Tsuk

*Racah Institute of Physics, The Hebrew University, Jerusalem, 91904, Israel*

## Abstract

In the framework of a gauge mediated quiver-like model, the standard model flavor texture can be naturally generated. The model – like the MSSM – has furthermore a region in parameter space where the lightest Higgs mass is fed by heavy stop loops, which in turn sets the average squark mass scale near 10 – 20 TeV. We perform a careful flavor analysis to check whether this type of mild-split SUSY passes all flavor constraints as easily as envisioned in the original type of split SUSY. Interestingly, it turns out to be on the border of several constraints, in particular, the branching ratio of  $\mu \rightarrow e\gamma$  and, if order one complex phases are assumed, also  $\epsilon_K$ , neutron and electron EDM. Furthermore, we consider unification as well as dark matter candidates, especially the gravitino. Finally, we provide a closed-form formula for the soft masses of matter in arbitrary representations of any of the gauge groups in a generic quiver-like model with a general messenger sector.

---

*latif.eliaz(at)mail.huji.ac.il*  
*giveon(at)phys.huji.ac.il*  
*gudnason(at)phys.huji.ac.il*  
*eitan.tsuk(at)mail.huji.ac.il*

# 1 Introduction

Supersymmetry is an elegant solution to the hierarchy problem of the standard model (SM). It is clear that some explanation as to why the Higgs is so light compared to the Planck scale is sought for in a fundamental theory of particle physics. What is less clear cut is how much fine-tuning to allow for in practice. Common lore is that ten percent is not “fine” tuning and the one-percent level is acceptable. The discussion of how big this number may be is somewhat philosophical and examples in Nature are known where a fine-tuning of the 0.1 per-mille level is realized; e.g. the binding energy of triplet deuteron is about  $\sim 2.2$  MeV which is only slightly above the energy released in neutron beta decay and is important because it prevented all the neutrons from decaying during the evolution of the Universe. Furthermore, the singlet state of deuteron does not exist; nevertheless, virtual particle exchange affects the neutron cross section, since the negative binding energy – only 60 keV – is very small. Naive expectations would set the deuteron binding energy of the order of a hundred MeV, but cancellation in the effective theory leaves the binding energy of both the singlet and the triplet states of order one MeV [1]. Since some degree of fine-tuning has been observed in Nature, we contemplate a more relaxed attitude towards fine-tuning, in the spirit of e.g. [2].

The hierarchy problem is not the only piece of the puzzle that one would wish be explained by the theory of Nature. Assuming that general relativity is correct at certain astrophysical scales (say at the kilo parsec scale), the existence of dark matter halos in for instance dwarf spheroidals is necessary for flattening the rotation curves of satellites. A popular candidate is a sufficiently weakly interacting massive particle (WIMP) of which cold dark matter (CDM) is made of. Certain supersymmetric extensions of the SM come with such a candidate with a mass and abundance compatible with observations. Furthermore, the electric charge is observed to be quantized and the standard model gauge couplings hint at gauge coupling unification, both of which calls for the possibility of a grand unified theory (GUT). Supersymmetry typically further enhances the precision to which this happens under certain conditions. Finally, the quark and lepton masses and mixing angles have a very particular form, which calls for some underlying mechanism.

In a series of works, following [3–5], we have considered a gauge mediated supersymmetric extension of the SM in which we double the SM gauge group and Higgs them back together at low energies by means of a link field attaining a VEV [6–10]. Our focus has been on the natural part of parameter space, i.e. keeping the stops as light as possible [10] and explaining all 18 parameters of the SM [9], satisfying the constraints coming from collider data and flavor physics. In the particular model we studied, we were able to obtain a natural model (i.e. fine tuning of parameters at the percent level at worst), which however has three short comings. The lightest supersymmetric particle (LSP), being the gravitino, is too light to be a CDM candidate and the embedding of the model into a unifying theory is not straightforward (some ideas regarding an elaboration that could do the job were put forward in [10]). The final short-coming is that even though the natural setting can avoid fine-tuning in the Higgs quartic, some degree of tuning is necessary in order for this type of model not to be at odds with CP-violating observables, like the  $\epsilon_K$  parameter of the kaon system.

If on the other hand, we relax our attitude towards the level of acceptable fine tuning, as in the spirit of split SUSY [11–13, 2]; say if we allow for a fine tuning at the 0.1–1 per-mille level for the Higgs quartic, then the same type of model as described above is able to still explain the 18 parameters of the SM, to provide a WIMP CDM candidate in terms of the gravitino (being much heavier than in the other scenario) and finally to unify without any elaborations of the model. The supersymmetric flavor problem is then addressed here simply by universality and decoupling; all the squarks will be heavier than about 10 TeV in order to amplify the Higgs quartic coupling for obtaining a 125 GeV Higgs.

In this paper, we focus on two branches of the above described model. In one case, supersymmetry breaking is mediated near the grand unified (GUT) scale and, in this case, unification as well as a gravitino

dark matter candidate can be contemplated. This case comes with a long renormalization running, which can potentially be probed in future experiments by certain flavor observables, e.g. the electric dipole moment (EDM) of the neutron and the branching ratio of  $\mu \rightarrow e\gamma$ . In the other case, supersymmetry breaking is mediated at a relatively low scale, i.e.  $\sim 10^{6-7}$  GeV, and it has a possible embedding in SQCD [14] as well as a light gravitino that could be contemplated as a warm dark matter candidate. Both scenarios have only gauginos and the gravitino sparticles at mass scales below  $\sim 1$  TeV, but are interestingly not far from constraints due to flavor observables, especially, the CP-violating ones. Future experiments, for e.g. the EDMs, will be able to probe considerable parts of their parameter spaces.

The paper is organized as follows. In sec. 2 we present an overview of the model without too many technical details. The reader can then skip to the discussion if not interested in further details. In secs. 3 and 4 we present the two branches of the model, with high- and low-scale mediation of SUSY breaking, respectively, and their corresponding spectra. In the high-scale case, we contemplate unification, which is analyzed in sec. 5. The flavor constraints for both model types are studied in detail in sec. 6. Then the prospects of gravitino dark matter is discussed in sec. 7 and finally, sec. 8 concludes with a discussion. In app. A, we provide a closed-form formula for the soft masses of matter in arbitrary representations of any of the gauge groups in a generic quiver-like model with a general messenger sector. App. B contains a Monte Carlo analysis of the diagonalization matrix elements entering the flavor constraints.

## 2 Overview of the model

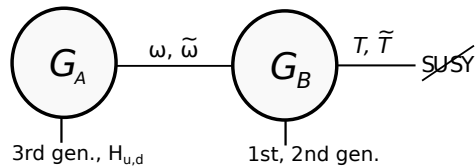


Figure 1: A diagram describing the model with gauge groups  $G_A, G_B = U(1) \times SU(2) \times SU(3)$  and link fields  $\omega, \tilde{\omega}$ . SUSY breaking is connected via messenger fields  $T, \tilde{T}$  only to  $G_B$ . We refer to the model as depicted above as the *normal model* while the *inverted model* has the matter content on the two nodes swapped, i.e. the 1st and 2nd generations are charged under node  $A$  while the 3rd generation and the Higgses are charged under node  $B$ .

The model of beyond-SM (BSM) physics we study in this paper is sketched in fig. 1 and is generically a non-flavor-blind extension in the class of gauge mediated supersymmetric models. The structure of the gauge groups is used to generate the SM flavor texture, which we will describe shortly.

The model is characterized by the following scales. Supersymmetry is broken in a secluded sector and mediated to the node  $B$  at the messenger scale  $M$ , which is taken roughly an order of magnitude lower than the Higgsing scale (of the link fields)  $\langle \omega \rangle = \langle \tilde{\omega} \rangle = v$ , viz. the VEV of the link fields. This means that at the messenger scale the theory is basically just a single node – i.e. an MSSM-like theory – at scale  $M$  with more structure at scale  $v > M$ . Further up in scale, we contemplate a UV completion with dynamics generating higher-dimension operators suppressed by the scale  $\Lambda_{\text{flavor}}$ , giving rise to fermion masses and SM flavor texture. Hence in this paper we are considering the part of the two-node parameter space where  $\Lambda_{\text{flavor}} > v > M$ . In sec. 3 and 4, we consider the messenger scale  $M$  to be near the GUT scale and near  $\sim 10^{6-7}$  GeV, respectively.

The matter content of the supersymmetric SM (SSM) is split on the two gauge groups  $G_A$  and  $G_B$  as follows: the complete third generation is charged under  $G_A$  together with the two Higgs superfields,  $H_u, H_d$ , giving a tree-level top-Yukawa of order one, while the first two generations sit on the other group

$G_B$ , giving vanishing Yukawas at tree-level. This explains why the top, bottom and tau have larger mass than the rest of the SM fermions. The representation of the link fields  $\omega, \tilde{\omega}$  determines the flavor texture of the SM fermions as we shall review next. We denote the model as just described by the *normal model*, whereas if we simply swap the matter content of the two gauge groups, we call it the *inverted model*, see fig. 1; such a swapping does not affect the flavor texture of the SM particles, though it does affect some aspects of flavor constraints.

## 2.1 Flavor texture

Summarizing the results of [9], the Yukawa matrices can be generated via higher-dimension operators like, for instance

$$\frac{\lambda_{ij}^2}{\Lambda_{\text{flavor}}^2} Q_i H_u u_j^c \omega_Q \omega_{u^c}, \quad i, j = 1, 2 \quad (\text{generation indices}). \quad (1)$$

Flavor texture is ideal for the choice of  $\omega$  ( $\tilde{\omega}$ ) transforming in the block-diagonal representation of  $(\mathbf{10}, \overline{\mathbf{10}})$  ( $(\overline{\mathbf{10}}, \mathbf{10})$ ). The  $\mathbf{10}$  decomposes like  $Q \oplus u^c \oplus e^c$  under  $U(1) \times SU(2) \times SU(3)$ , where the labels refer to the representations  $R$  of the SM fields. Assuming order-one coefficients of the higher-dimension operators, this representation gives rise to the following Yukawa textures [9]

$$Y^u \sim \begin{pmatrix} \epsilon^2 & \epsilon^2 & \epsilon \\ \epsilon^2 & \epsilon^2 & \epsilon \\ \epsilon & \epsilon & 1 \end{pmatrix}, \quad Y^d \sim \begin{pmatrix} \epsilon^2 & \epsilon^2 & \epsilon \\ \epsilon^2 & \epsilon^2 & \epsilon \\ \epsilon^2 & \epsilon^2 & 1 \end{pmatrix}, \quad Y^e \sim \begin{pmatrix} \epsilon^2 & \epsilon^2 & \epsilon^2 \\ \epsilon^2 & \epsilon^2 & \epsilon^2 \\ \epsilon & \epsilon & 1 \end{pmatrix}, \quad (2)$$

with  $\epsilon = \epsilon_Q = \epsilon_{u^c} = \epsilon_{e^c}$  being the ratio

$$\epsilon_R = \frac{\langle \omega_R \rangle}{\Lambda_{\text{flavor}}} \sim \frac{1}{10}. \quad (3)$$

The textures roughly make the following prediction

$$\frac{m_c}{m_t} \sim \frac{m_s}{m_b} \sim \frac{m_\mu}{m_\tau} \sim \mathcal{O}(\epsilon^2), \quad \frac{m_t}{m_b} \sim \frac{m_t}{m_\tau} \sim \tan \beta. \quad (4)$$

The numerical value is hence determined from the observed quark masses and if  $\tan \beta$  is sizable, the top-bottom mass hierarchy is generated naturally. The above pattern reproduces the quark and lepton masses as well as the measured CKM matrix with coefficients in the range [0.8–1.1] for  $\tan \beta = 40$ , see [9]. Here, however, we will not insist on such a high degree of precision.

The off-diagonal elements of the Yukawas are crucial in order to produce a sufficient amount of quark mixing, and therefore  $\epsilon$  of order 1/10 is preferred. This fixes the Higgsing scale in terms of the flavor scale:  $v = \langle \omega \rangle \sim \Lambda_{\text{flavor}}/10$ .

## 2.2 The Higgs and gravitino masses

The Higgs boson has been found at the LHC with a mass of 125–126 GeV [15, 16] and hence we need to accommodate such a “large” Higgs quartic in the model. In the part of parameter space chosen in the present model (viz.  $v > M$ ), the D-terms associated with the enhanced gauge symmetry are decoupled and do not give any observable contribution to the Higgs quartic coupling. Also, because we are using gauge mediation, the trilinears vanish at the messenger scale and are nowhere near sizable enough for increasing the Higgs mass with light squarks. Hence, the simplest possibility, which we utilize in this

model, is having very heavy sfermions, in particular, we need the stops of order  $\sim 10$  TeV, which will feed mass at one loop to the Higgs as [17]

$$\delta m_{h_0}^2 = \frac{3}{4\pi^2} \cos^2(\alpha) Y_t^2 m_t^2 \log\left(\frac{m_{\tilde{t}_1} m_{\tilde{t}_2}}{m_t^2}\right), \quad (5)$$

where  $\alpha$  is the Higgs mixing angle [17],  $Y_t$  is the top Yukawa,  $m_t$  is the top mass and finally  $m_{\tilde{t}_{1,2}}$  are the stop masses.

This means that the scale of the soft masses is  $\sqrt{2}\alpha F/(4\pi M) \sim 10$  TeV. Hence, in the high-scale mediation case, where  $M \sim 10^{15}$  GeV, we have roughly

$$\sqrt{F} \sim 3 \times 10^{10} \text{ GeV}, \quad (6)$$

and in turn  $x \equiv F/M^2 \sim 8 \times 10^{-11}$  giving a gravitino mass of roughly

$$m_{3/2} \gtrsim 20 \text{ GeV}, \quad (7)$$

which is suitable as a cold dark matter candidate. In the low-scale mediation case on the other hand, the gravitino will be much lighter and can at best be a warm dark matter candidate, see sec. 7.2. The above calculated value assumes  $k \equiv F/F_0 = 1$ , where  $\sqrt{F}$  is the SUSY-breaking scale felt by the messenger field whereas  $\sqrt{F_0}$  is the SUSY-breaking scale determining the gravitino mass (though  $k \leq 1$  and could be  $\ll 1$  [18, 19]).

### 2.3 Messenger sector, soft masses and the sparticle spectrum

In order to get reasonably light gaugino masses compared to the necessarily very heavy sfermion masses, we choose to work with a messenger sector having more than one pair of messengers. For concreteness, we choose a messenger sector having two messengers (times an integer  $p$ , which has a trivial impact on the gaugino mass to sfermion mass ratio)

$$\int d^4\theta \left( T_i^\dagger T_i + \tilde{T}_i^\dagger \tilde{T}_i \right) + \int d^2\theta \tilde{T}_i \tilde{\mathcal{M}}_{ij} T_j + \text{c.c.}, \quad \tilde{\mathcal{M}} = \mathbf{1}_p \otimes \mathcal{M}, \quad \mathcal{M}_{ab} = m_{ab} + S\lambda_{ab}, \quad (8)$$

where  $i, j = 1, \dots, 2p$ ,  $p \in \mathbb{Z}_{>0}$ ,  $a, b = 1, 2$  and the SUSY-breaking spurion attains an F-term VEV

$$\langle S \rangle = \theta^2 F, \quad (9)$$

and we assume messenger parity as well as CP conservation in the messenger sector. The above is a messenger sector characterized by a two-by-two matrix  $\mathcal{M}$  whose determinant specifies whether the gaugino masses vanish two leading order or not [20]. Namely, if  $\det \mathcal{M}$  is independent of  $S$ , then the gaugino masses vanish to leading order in SUSY breaking. We consider such a case in sec. 4 while in sec. 3 we study a case where the gaugino mass does not vanish to leading order in SUSY-breaking and thus allowing for a high messenger scale  $M$ , suitable for a single scale unification scenario. The sparticle spectrum, obtained via RG evolution down to the weak scale, is presented for two corresponding benchmark points in figs. 2 and 3.

### 2.4 Flavor constraints

The way the supersymmetric flavor problem is tackled in this type of mild-split models is by degeneracy. In the limit of the Higgsing scale,  $m_v^2 \equiv 2(g_A^2 + g_B^2)v$ , being much larger than the messenger scale,  $m_v \gg M$ , universality of the squark masses holds true. On the other hand, we would like to have as few scales in

the model as possible, that is, if  $m_\nu$  would be of the order of  $M$  (but still larger), we would think of this as being “one scale.” Furthermore, the scale  $M$  determines the gravitino mass, which in turn determines whether the model can have a neutralino LSP or only a gravitino LSP. This is important for the dark matter candidate in question. In order to make a quantitative assessment of the necessary separation of scales  $m_\nu, M$ , we perform an extensive analysis of flavor constraints in sec. 6. The result of many sflavor checks is that the  $K - \bar{K}$  meson mixing with double insertion in the mass insertion (MI) approximation is the most important of the meson mixings with respect to the mass splitting induced at the messenger scale. The  $D - \bar{D}$  meson mixing, however, at double insertions is sensitive to the top-Yukawa induced splitting for large RG evolution. The bottom meson mixings are subdominant to the mentioned ones. The branching ratio for  $b \rightarrow s\gamma$  is potentially important. However, due to vanishing  $A$ -terms,  $\delta^{\text{LR}}$  is not inducing any sizable flavor changing effects. The branching ratio of  $\mu \rightarrow e\gamma$  is one of the major constraints and with a future experimental upgrade, it has potential to probe quite far in the parameter space of the model. The EDM coming both from gluino/squark diagrams and from the slepton sector are important if no assumptions are made about complex phases. Again with future experimental limits, the EDM of the electron will be able to probe much farther in parameter space. Finally, let us mention that the constraints due to the CP-violating observable  $\epsilon_K$  can also be satisfied with no assumption of alignment in the high-scale model of sec. 3 with inverted matter content.

## 2.5 Results

Setting the gluino mass near 1150 GeV – its present bound [21], the sparticle spectrum that we found then depends mainly on the choice of  $\tan\beta$  and the messenger scale. The average squark masses weigh in at about 12+ TeV and the slepton masses at about 7+ TeV. The wino is near 400 GeV and the bino sits near 200 GeV. The gravitino is almost always the LSP, although the bino can be lighter in a corner of parameter space, see shortly. Two benchmark points are presented in figs. 2 and 3, for the high-scale and low-scale models, respectively.

We have made a simple one-loop estimate to see how well the high-scale model unifies. It turns out to match the measured value of the strong coupling only at the  $2 - 3\sigma$  level. However, two-loop effects, threshold effects and more importantly, matter from the link sector has not been taken into account, which for just a slight splitting could alter this substantially.

The flavor constraints can be satisfied, although some of the constraints are on the border of probing the model, depending on whether the normal or the inverted quiver model is chosen. Even with order one complex phases, the models pass more or less the limit on the  $\epsilon_K$  CP-violating parameter of the kaon system as well as constraints from the electric dipole moments of the neutron and electron.

The high-scale model has a gravitino dark matter candidate in most of the parameter space, although a bino LSP is possible in a corner. The gravitino is a cold dark matter candidate and can account for all the measured dark matter abundance in accord with the recent observation of Planck with a not-too-low reheating temperature to even be compatible with a leptogenesis scenario. A potential problem, however, is due to the NLSP – the bino, decaying along with the emitted photons potentially destroying light nuclei, synthesized during BBN. There are some assumptions built into such cosmological calculations and we have quoted a couple of ways out in sec. 7.

In the low-scale mediation case, which can be embedded in a dynamical model, the gravitino could potentially be a warm dark matter candidate. We leave the verdict of the validity of such a possibility to the astrophysics community.

In conclusion, we have presented a model with two different incarnations, that address *all* the SM parameters, with the measured Higgs mass. It is able to pass sflavor constraints, it may have perturbative unification, and it has possibilities for providing a dark matter candidate.

## 2.6 Reading on

In the following sections we will go into detail with the two different model choices, their parameter spaces (secs. 3 and 4), and then in turn their flavor constraints (sec. 6) and dark matter prospectives (sec. 7). For the high-scale case we contemplate also the quality of unification in sec. 5. In app. A we give two-loop mass formulae for the scalars in a generic quiver with a general messenger sector. The reader not interested in further details can take a look at the spectra of figs. 2 and 3 as well as at the summary plot 12 for the sflavor constraints and then jump to the discussion (sec. 8).

## 3 A high-scale model

This model is chosen as an example of mild-split SUSY which enjoys gauge coupling unification and a gravitino dark matter candidate, though it does not come from a manifest dynamical embedding (but perhaps an embedding in some ‘uplifted vacuum’ exists). The reason is the following. Generic dynamical embeddings have vanishing gaugino masses to leading order in SUSY breaking [20], unless the theory sits in an ‘uplifted vacuum’ of the type studied e.g. in [22, 23]. Here, since we take the messenger scale  $M$  to be near the GUT scale, a messenger sector having vanishing gaugino masses to leading order cannot produce a viable phenomenology. The leading order gaugino mass goes like  $Mx$ , where  $x \equiv F/M^2$ , while the next-to-leading order contribution can be shown to go like  $Mx^3$ , which for  $x \sim 10^{-10}$  is completely negligible even for  $M$  at the GUT scale. Therefore, we consider here a different messenger sector which interpolates that of minimal gauge mediation (MGM) (with two messengers) and that of the dynamical embedding by a single real parameter  $\alpha$

$$\mathcal{M} = M \begin{pmatrix} 1 - 2\alpha & 0 \\ 0 & 1 \end{pmatrix} + S \begin{pmatrix} 1 & \alpha \\ \alpha & 1 \end{pmatrix}. \quad (10)$$

For  $\alpha = 1$  the determinant is  $-M^2$ , i.e. independent of  $S$  and hence due to the results of [20], the gaugino masses vanish to leading order in SUSY breaking. For vanishing  $\alpha$ , on the other hand, the messenger sector is that of MGM with two messenger fields. This interpolation is very simple, but has a sick region, namely  $\alpha$  should not be taken to be near  $1/2$  as one of the fermionic messengers is massless (or very light) and hence the phenomenology is not viable in that region. Since we are interested in a mild-split SUSY scenario, we consider  $\alpha$  less than, but close to, unity.<sup>1</sup>

The gaugino masses for this particular messenger sector are given by

$$m_{\tilde{g},k} = \frac{\alpha_k}{4\pi} Mx \, 2p \frac{1 - \alpha}{2\alpha - 1} + \mathcal{O}(\alpha_k Mx^3), \quad \alpha \in [0, 1], \quad (11)$$

where  $\alpha_k \equiv g_k^2/(4\pi)$  are the gauge couplings with  $k = 1, 2, 3$  corresponding to  $U(1)_Y, SU(2)_L, SU(3)_c$ , respectively, and  $x \equiv F/M^2$ . Notice that for  $\alpha = 1$  the above expression vanishes and for  $\alpha = 0$  the standard MGM formula is formally recovered (up to the minus sign) with Dynkin index  $2p$ , corresponding to  $2p$  messengers. Note also that the expression is not valid for  $\alpha = 1/2$ .

The sfermion masses are given by

$$m_{\tilde{f}}^2 = 2 \sum_{k=1}^3 \left( \frac{\alpha_k}{4\pi} \right)^2 C_{\tilde{f},k} M^2 x^2 p \left( 1 + \frac{1}{(1 - 2\alpha)^2} + \frac{\alpha \log |1 - 2\alpha|}{\alpha - 1} \right) + \mathcal{O}(\alpha_k^2 M^2 x^4), \quad (12)$$

where  $C_{\tilde{f},k}$  is the quadratic Casimir of the sfermion  $\tilde{f}$  with respect to the gauge group  $k$ . In the limit of  $\alpha \rightarrow 1$ , the above expression is formally equal to that of MGM with Dynkin index  $4p$ , whereas for  $\alpha = 0$  it recovers MGM with Dynkin index  $2p$ , corresponding to  $2p$  messengers.

<sup>1</sup>This type of mild-split SUSY spectrum comes also naturally in axion mediation models, see e.g. [24].

The given masses are all calculated at the messenger scale  $M$  and need to be RG evolved down to the electroweak scale for the physical low-energy spectrum from which we can understand the phenomenology of the model. Since we work in the part of parameter space where the two-nodes quiver-like model effectively is MSSM-like, we can directly use the spectrum calculator SOFTSUSY 3.3.4 [25].

In our model, the gluino mass is a(n) (almost) free parameter, so we set it at 1150 GeV, which is close to current exclusion limits from the LHC, see e.g. [21]. The other gaugino masses follow approximately from the GUT relation. If the bino were lighter than about 100 GeV, the charged wino would be excluded up to  $\sim 315$  GeV by ATLAS for decoupled sleptons [26]. However, for a bino heavier than around 120 GeV, there is practically no bound from the LHC, although Tevatron data still excludes such a charged wino below 270 GeV [27]. Due to the GUT relation among the gaugino masses, the exclusion limits on the charged wino and on the bino are automatically satisfied when the bound on the gluino is satisfied.

We show a benchmark point in fig. 2. The shown low-energy spectrum consists basically of the lightest CP-even Higgs at 125.5 GeV [28]<sup>2</sup> and the bino, wino and gluino around 192 GeV, 383 GeV and 1150 GeV, respectively. The LSP is the gravitino with a mass bigger than 28 GeV and the fine-tuning according to the Barbieri-Giudice measure [30]

$$\Delta_\mu \equiv \frac{2|\mu|^2}{m_Z^2}, \quad (13)$$

is roughly  $\Delta_\mu^{-1} \sim 0.1$  per-mille. In the chosen benchmark point, we have set  $\tan\beta = 20$  in order to naturally produce a top-bottom hierarchy in the SM fermion mass sector and the lightest CP-even Higgs is set at 125.5 GeV which then fixes the stop masses and by means of the chosen parameter space also the rest of the sfermions.

The scales of the average squark masses and the gravitino mass are

$$\tilde{m}_L \sim 13.5_{-2.4}^{+3.4+5.2+1.1}_{-3.1-0.93} \text{ TeV}, \quad \tilde{m}_R \sim 11.4_{-2.1}^{+2.9+4.4+0.94}_{-2.6-0.80} \text{ TeV}, \quad m_{3/2} \gtrsim 28.4_{-5.4-6.8}^{+7.6+11.5+2.3}_{-2.0} \text{ GeV},$$

where the first uncertainty is estimated from changing the lightest Higgs mass by  $\pm 0.585$  GeV which corresponds to  $\pm 1\sigma$ , statistical and systematical combined, and the second is due to the uncertainty in the measurement of the top mass, i.e.  $\mp 1$  GeV corresponding to  $\mp 1\sigma$ , combined. The last uncertainty is estimated by changing the strong coupling  $\alpha_3$  by  $\pm 1.1 \times 10^{-3}$  corresponding to  $\pm 1\sigma$ , experimentally.

One can however ask what happens to the spectrum by lowering  $\tan\beta$ , since some tuning of the top-bottom hierarchy is acceptable. What happens when keeping the Higgs fixed at 125.5 GeV and the gluino at 1150 GeV (near the bound), is that the squarks become heavier. With these constraints and of course asserting electroweak symmetry breaking, the mean squark masses raise to  $\tilde{m}_L \sim 36$  TeV,  $\tilde{m}_R \sim 31$  TeV,  $m_{3/2} \sim 79$  GeV for  $\tan\beta = 7$  and to  $\tilde{m}_L \sim 144$  TeV,  $\tilde{m}_R \sim 117$  TeV,  $m_{3/2} \sim 307$  GeV, for  $\tan\beta = 5$ , see fig. 4. We have not been able to find a spectrum with a heavy enough Higgs for  $\tan\beta \lesssim 5$  for fixed gluino mass, due to problems of convergence of the numerical calculation. We have been able to find spectra with  $\tan\beta \lesssim 5$  by raising the gluino mass, but as we are investigating the scenario with a gluino as close to discovery as possible we do not consider further such possibility.

We have calculated the branching ratios of the spectrum in fig. 2 using SUSY-HIT [31] and found the following SUSY decays shown in tab. 1. A typical split-SUSY decay is the gluino decaying into a gravitino and a gluon [13]. This is, however, too suppressed in this type of mild-split model to have any phenomenological consequence. In this particular spectrum the branching ratio for such a decay is about  $2 \times 10^{-21}$ . The production modes in this model will be via Drell-Yan production of either  $\widetilde{W}^+\widetilde{W}^-$  or  $\widetilde{W}^0\widetilde{W}^\pm$  [32]. As can be read off from tab. 1, the neutral wino decays almost exclusively to a bino via Higgs emission while the bino decays dominantly into a photon and a gravitino. Due to the mentioned

---

<sup>2</sup>For recent fits to the Higgs mass, see e.g. [29] in which a lower face-value is obtained. In order to be conservative, we choose to stick with a higher Higgs mass as a worst-case-scenario.



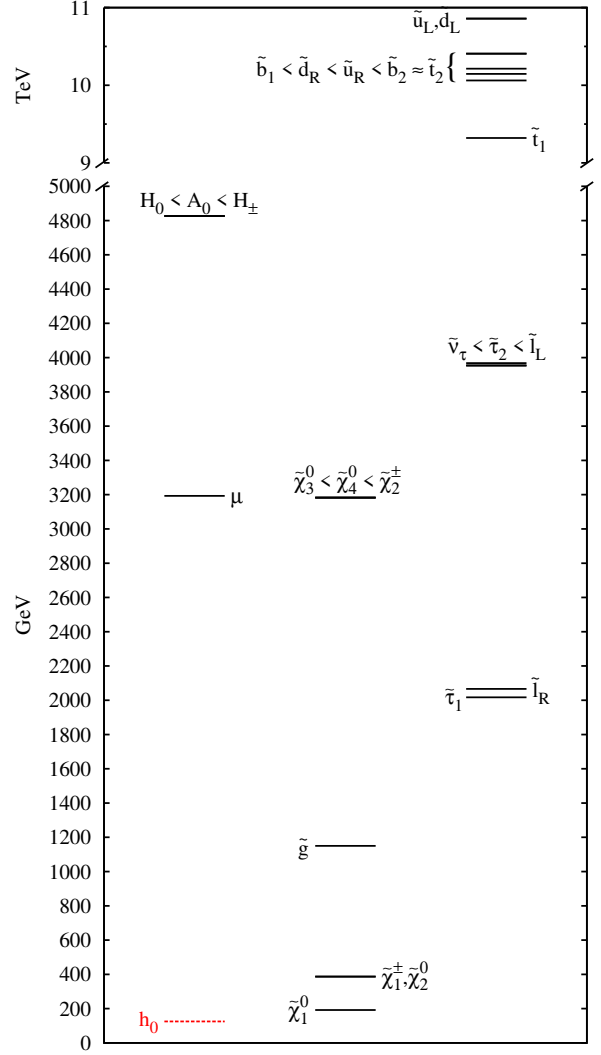
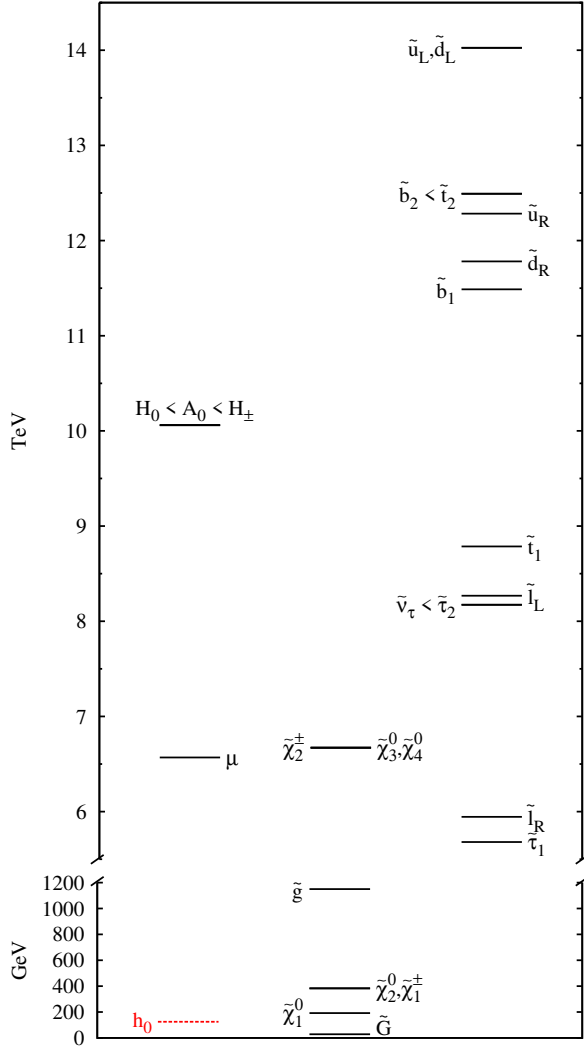


Figure 2: Benchmark point for the high-scale model with  $M = 1.15 \times 10^{14}$  GeV,  $x = 8.97 \times 10^{-9}$ ,  $p = 1$ ,  $y = 35$ ,  $\alpha = 0.941$ ,  $\tan \beta = 20$ ,  $\Delta_\mu^{-1} = 9.6 \times 10^{-5}$ .

Figure 3: Benchmark point for the low-scale model with  $M = 1.61 \times 10^6$  GeV,  $x = 0.850$ ,  $p = 1$ ,  $z = 1$ ,  $\tan \beta = 20$ ,  $\Delta_\mu^{-1} = 4.1 \times 10^{-4}$ .

gluino $\rightarrow$	Br (high-scale)	Br (low-scale)
$\tilde{B}t\bar{t}$	18.7%	5.5%
$\tilde{B}q\bar{q}$ , $q = u, c$	7.9%	6.2%
$\tilde{W}^+b\bar{t}$ or c.c.	7.2%	7.9%
$\tilde{W}^+q\bar{p}$ , $(q, p) = (d, u), (s, c)$ or c.c.	6.0%	8.8%
$\tilde{W}^0b\bar{b}$	4.7%	5.2%
$\tilde{W}^0q\bar{q}$ , $q = u, d, c, s$	3.0%	4.4%
$\tilde{B}b\bar{b}$	2.9%	1.9%
$\tilde{B}q\bar{q}$ , $q = d, s$	2.5%	1.8%
$\tilde{W}^0t\bar{t}$	2.5%	2.7%
$\tilde{B}g$	0.013%	$1.1 \times 10^{-5}$
$\tilde{W}^0g$	$8.3 \times 10^{-8}$	$9.5 \times 10^{-7}$
$\tilde{G}g$	$2.0 \times 10^{-21}$	$2.2 \times 10^{-6}$
charged wino $\rightarrow$	Br	Br
$\tilde{B}W^+$	100%	100%
$\tilde{G}W^+$	$2.4 \times 10^{-24}$	$1.0 \times 10^{-9}$
neutral wino $\rightarrow$	Br	Br
$h\tilde{B}$	99%	96%
$Z\tilde{B}$	1.4%	3.8%
$Z\tilde{G}$	$1.1 \times 10^{-24}$	$6.5 \times 10^{-10}$
$\gamma\tilde{G}$	$7.4 \times 10^{-25}$	$2.9 \times 10^{-10}$
$h\tilde{G}$	$2.8 \times 10^{-31}$	$3.0 \times 10^{-15}$
bino $\rightarrow$	Br	Br
$\gamma\tilde{G}$	84%	89%
$Z\tilde{G}$	16%	11%
$h\tilde{G}$	$2.6 \times 10^{-9}$	$4.8 \times 10^{-8}$

Table 1: Branching ratios of selected SUSY decays calculated using SUSY-HIT [31]. The above estimates for the branching ratios do not include the flavor violating decays that are present in our model, as they in turn depend on the parameter space of the model.

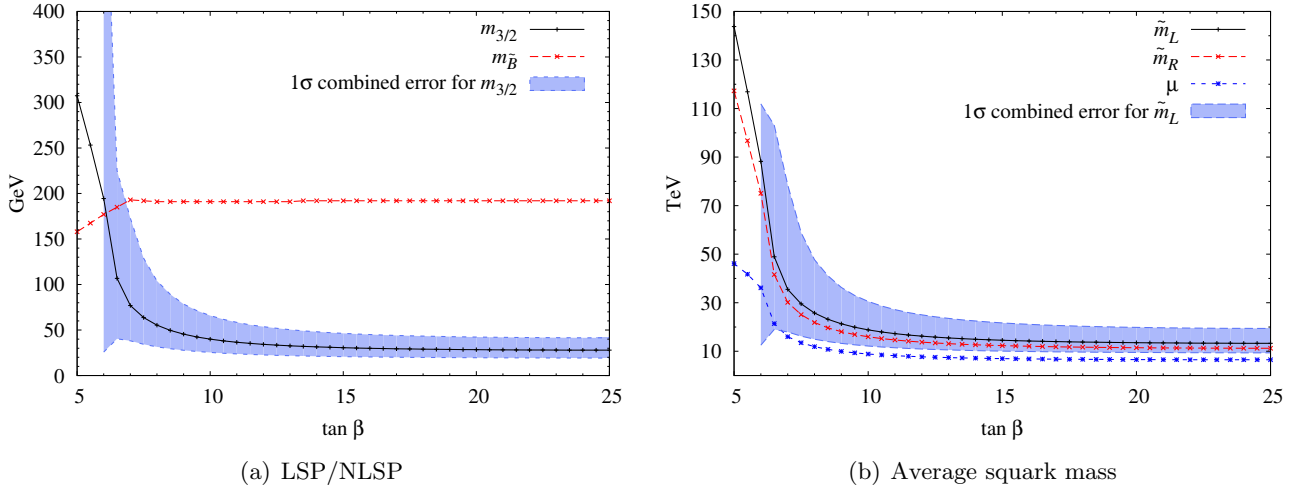


Figure 4: a) The LSP/NLSP and b) the average squark masses as functions of  $\tan\beta$  for the high-scale model. The plots are made keeping the Higgs mass fixed at 125.5 GeV and the gluino mass at 1150 GeV. The relation between  $\tilde{m}$  and  $\tan\beta$  is sensitive to the uncertainties in  $m_t, m_h$  and  $\alpha_3$ . The  $1\sigma$  areas show the combined errors on the gravitino mass and on the left-handed average squark mass, respectively. The combined error is calculated by adding each error in quadrature, i.e.  $\pm\sqrt{\Delta_{\mp t}^2 + \Delta_{\pm h}^2 + \Delta_{\pm\alpha_3}^2}$ . The errors are very large for  $\tan\beta < 6$  and are not shown here.

Higgs emission, one should consider search strategies of [33] and due to the charged wino decays, also searches for opposite-sign dilepton+missing transverse energy are potentially important [34].

## 4 A low-scale model

Here we study a low-scale model which does not allow for conventional gauge coupling unification, but instead it has a known dynamical embedding in a deformed  $SU(N)$  SQCD [14, 8] with an appropriate number of flavors. In particular, the messenger sector is a specific outcome of the above mentioned scenario [14, 8]

$$\mathcal{M} = M \begin{pmatrix} z & 1 \\ 1 & 0 \end{pmatrix} + S \begin{pmatrix} 1 & 0 \\ 0 & 0 \end{pmatrix}. \quad (14)$$

The explicit formulae for the gaugino masses and the sfermion masses are given in [35, 36, 8]; specifically we will use the parametrization given in [8].

A benchmark point for this model is shown in fig. 3. The low-energy spectrum is similar to the high-scale model and it consists of the lightest CP-even Higgs at 125.5 GeV and the bino, wino and gluino around 192 GeV, 387 GeV and 1150 GeV, respectively. The LSP is the gravitino with a mass bigger than 0.53 keV, which is slightly too large with respect to the bound from overclosure of the Universe, see fig. 5. The fine-tuning, however, according to the Barbieri-Giudice measure is slightly better than in the high-scale case, viz. 0.4 per-mille. As in the high-scale case, we have chosen  $\tan\beta = 20$  in order to produce a top-bottom hierarchy in the SM fermion mass sector and the lightest CP-even Higgs is set at 125.5 GeV which then fixes the stop masses and by means of the chosen parameter space also the rest of the sfermions. The main difference in this spectrum with respect to that of the high-scale model, is

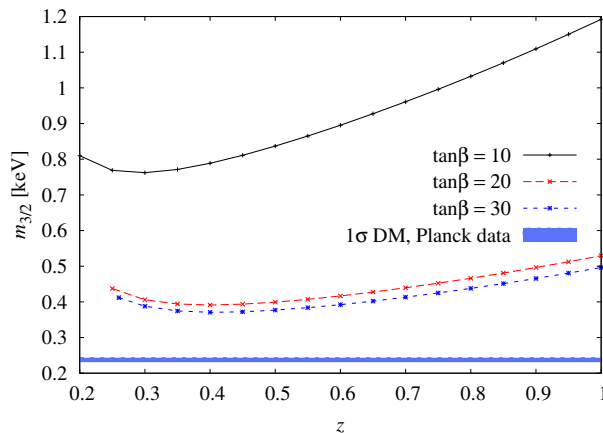


Figure 5: Gravitino mass in the low-scale model as function of the parameter  $z$ . The messenger scale  $M$  and  $x$  are fixed by setting the Higgs and gluino masses equal to 125.5 GeV and 1150 GeV, respectively. The left-most end-point of each curve is approximately where  $x$  approaches unity (recall that  $x \leq 1$  in order not to have tachyonic messengers). We do not present the according change in the average mass of the squarks as it varies only about 1.5% with  $z$  in the range of the graph.

the mass of gravitino and that the sfermions, in particular the Higgsini, are somewhat lighter than in the high-scale case. The branching ratios for the spectrum in fig. 3 are calculated using SUSY-HIT [31] and shown in tab. 1.

## 5 Unification

In this section we will briefly discuss the degree to which gauge coupling unification works out in the high-scale mediation case. We will just make a one-loop estimate of the state of affairs and we will not incorporate a possible splitting in the link sector here. Defining the unification scale by the intersection of the U(1) and SU(2) gauge couplings, we can trace back the gauge coupling of SU(3) and compare it to the experimentally measured value at the scale of the  $Z$  mass. The expression at one-loop is independent of complete SU(5) multiplets and reads

$$\begin{aligned}
\alpha_3^{-1}(m_Z) \simeq & \alpha_1^{-1}(m_Z) - \frac{b_3^g}{2\pi} \log m_Z - \frac{b_3^{\tilde{g}}}{2\pi} \log m_{\tilde{g}} + \frac{b_1^h}{2\pi} \log m_H + \frac{b_1^{\tilde{h}}}{2\pi} \log \mu \\
& + \frac{b_3^g + b_3^{\tilde{g}} - b_1^h - b_1^{\tilde{h}}}{b_2^g + b_2^{\tilde{g}} + b_2^h + b_2^{\tilde{h}} - b_1^h - b_1^{\tilde{h}}} \left( \alpha_2^{-1}(m_Z) - \alpha_1^{-1}(m_Z) + \frac{b_2^g}{2\pi} \log m_Z + \frac{b_2^{\tilde{g}}}{2\pi} \log m_{\tilde{W}} \right. \\
& \left. + \frac{b_2^h - b_1^h}{2\pi} \log m_H + \frac{b_2^{\tilde{h}} - b_1^{\tilde{h}}}{2\pi} \log \mu \right), \tag{15}
\end{aligned}$$

where  $m_Z$ ,  $m_{\tilde{g}}$ ,  $m_{\tilde{W}}$ ,  $m_H$  and  $\mu$  are the  $Z$  mass, the gluino mass, the wino mass, the mass of the heavy Higgses and the higgsino mass, respectively, and  $b_3^g = -11$ ,  $b_3^{\tilde{g}} = 2$ ,  $b_2^g = -22/3$ ,  $b_2^{\tilde{g}} = 4/3$ ,  $b_2^h = 1/3$ ,  $b_2^{\tilde{h}} = 2/3$ ,  $b_1^h = 1/5$  and  $b_1^{\tilde{h}} = 2/5$ . In fig. 6 is shown the degree to which gauge coupling unification works in terms of the strong gauge coupling matching with the experimental measured value. If, for instance, the strong gauge coupling should match up with its experimentally measured value at  $m_Z$  to within  $2\sigma$ , the heavy Higgses should weigh less than about 4.7 TeV. Comparing with fig. 4,  $\alpha_3(m_Z)$  matches its

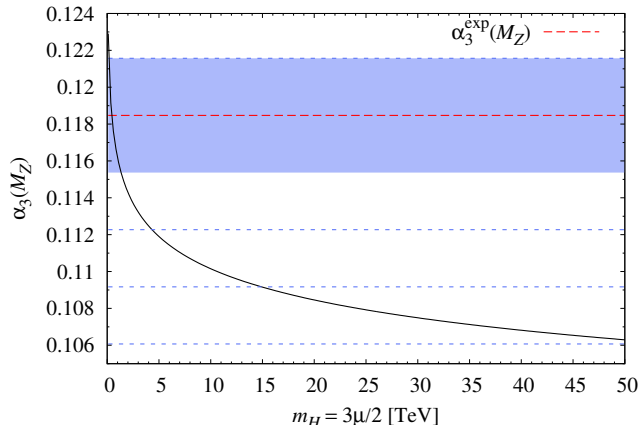


Figure 6: Unification at one loop is estimated by the intersection of the U(1) and SU(2) gauge couplings and then the SU(3) gauge coupling is traced back to the  $m_Z$ -scale where it is compared to the experimental value of [37]. The blue strip denotes the  $1\sigma$  band while blue-dashed lines show the 2–4 standard deviations from top to bottom. We use 0.0031 as the standard deviation, which is a combined value. We have set  $\mu = \frac{2}{3}m_H$ ,  $m_{\tilde{g}} = 1150$  GeV and  $m_{\tilde{W}} = 383$  GeV as a representative example using the spectrum of fig. 2.

experimental value between 2 and  $4\sigma$ s, depending on the value of  $\tan\beta$  and hence the scale of Higgses and higgsinos.

The gauge coupling unification described here is solely that of gauge group  $G_A$  of fig. 1 and it is not spoiled by the (un)Higgsing with the gauge group  $G_B$  as long as the gauge couplings on  $G_B$  are kept SU(5) invariant and the messenger and link fields transform in complete SU(5) representations.

## 6 Superpartner flavor and CP phases

In this section, we will explain the sflavor constraints in detail. Many constraints were checked that were subdominant and those are just mentioned with references to the literature whilst the important ones for the model are explained here (for reviews, see e.g. [38, 39]). As the model has near-flavor universality, it is adequate to use the Mass Insertion (MI) approximation [40]. Because the first two generations of squarks are on the same node, one could naively expect the  $K - \bar{K}$  and  $D - \bar{D}$  constraints to be automatically satisfied, whilst the constraints from  $B_d - \bar{B}_d$  (and  $B_s - \bar{B}_s$  to a lesser extent) to be important. It turns out, however, that the gluino box diagrams contributing to the mass difference in the neutral kaon system – even though having vanishing contributions from single flavor-flip insertions – have dominating/competitive contributions from double flavor-flip mass insertions  $(2 \rightarrow 3) \times (3 \rightarrow 1)$  [41]. This type of effective mass-insertion has recently received attention due to much interest in natural SUSY models with a hierarchy in the soft masses [42–47]. Even though we do not have a hierarchy in the soft masses, only an SU(2) flavor symmetry is preserved at the messenger scale in the two-nodes model and thus the mass differences – although small – resides between the first two and the third generation of squarks. This explains the importance of the double flavor-flip effective mass insertions. The reason why the kaon system is competitive with the  $B$  meson system, is due to the tighter experimental limit.

The meson mixing itself does not pose the strongest limit on the model at hand, but the CP-violating parameter  $\epsilon_K$  in the kaon system provides one of the toughest constraints.

Flavor violation is possible also in the leptonic sector where the branching ratio of  $\mu \rightarrow e\gamma$  gives rise

to strong constraints, especially for large  $\tan\beta \gtrsim 20 - 30$ . If furthermore order one complex phases – of which our model has two of – are not tuned away somehow, then the electric dipole moment of the electron sets an even stronger constraint. Finally, allowing for order one complex phases, also the squark sector induces electric dipole moments, in this case, affecting that of the neutron.

We will start by explaining the sflavor constraint calculation for the  $K - \bar{K}$  meson mixing and CP-violation, in order to set a limit on how small  $y = m_v/M$  can be;  $m_v^2 \equiv 2(g_A^2 + g_B^2)v^2$  is the Higgsing scale of the link fields  $\omega, \tilde{\omega}$ .<sup>3</sup> We work in the framework of the effective Hamiltonian

$$\mathcal{H}_{\text{eff}} = C_1 O_1 + \tilde{C}_1 \tilde{O}_1 + C_4 O_4 + C_5 O_5, \quad (16)$$

where the operators are defined as

$$O_1 = (\bar{d}_L^\alpha \gamma_\mu s_L^\alpha)(\bar{d}_L^\beta \gamma^\mu s_L^\beta), \quad O_4 = (\bar{d}_R^\alpha s_L^\alpha)(\bar{d}_L^\beta s_R^\beta), \quad O_5 = (\bar{d}_R^\alpha s_L^\beta)(\bar{d}_L^\beta s_R^\alpha), \quad (17)$$

with  $\alpha, \beta$  being color indices and  $\tilde{O}_1$  is given by  $O_1$  with  $L \rightarrow R$ . Since we are working in a gauge-mediated SUSY-breaking model with negligible  $A$ -terms, the operators  $O_{2,3}$  and their corresponding tilded ones are subdominant. The double flavor-flip mass insertion [41] contributions from gluino box diagrams have Wilson coefficients [40, 48, 49] given by [50]

$$\begin{aligned} C_1^{\tilde{g}} &\simeq -\frac{\alpha_3^2}{\tilde{m}^2} [(\delta_d^{LL})_{23}(\delta_d^{LL})_{31}]^2 g_1^{(3)}(x_{\tilde{g}}), \\ C_4^{\tilde{g}} &\simeq -\frac{\alpha_3^2}{\tilde{m}^2} [(\delta_d^{LL})_{23}(\delta_d^{LL})_{31}(\delta_d^{RR})_{23}(\delta_d^{RR})_{31}] g_4^{(3)}(x_{\tilde{g}}), \\ C_5^{\tilde{g}} &\simeq -\frac{\alpha_3^2}{\tilde{m}^2} [(\delta_d^{LL})_{23}(\delta_d^{LL})_{31}(\delta_d^{RR})_{23}(\delta_d^{RR})_{31}] g_5^{(3)}(x_{\tilde{g}}), \end{aligned} \quad (18)$$

where  $x_{\tilde{g}} \equiv m_{\tilde{g}}^2/\tilde{m}^2$ ,  $\tilde{m}$  being the average squark mass,  $m_{\tilde{g}}$  the gluino mass, and the loop functions are given in app. A of [50].

Another contribution to the  $K - \bar{K}$  mixing comes from double neutral Higgs penguin diagrams, again at fourth order in squark MIs [50]

$$C_4^H \simeq -\frac{\alpha_3^2 \alpha_2}{4\pi} \frac{m_b^2}{2m_W} \frac{\tan^4 \beta}{(1 + \epsilon_{\tilde{g}} \tan \beta)^4} \frac{|\mu|^2 m_{\tilde{g}}^2}{m_A^2 \tilde{m}^4} (\delta_d^{LL})_{23}(\delta_d^{LL})_{31}(\delta_d^{RR})_{23}(\delta_d^{RR})_{31} h_2^2(x_{\tilde{g}}), \quad (19)$$

where  $m_b$ ,  $m_W$ ,  $\mu$ ,  $m_A$  and  $\tilde{m}$  are the masses of the bottom quark, the  $W$ -bosons, the supersymmetric Higgs mass, the CP-odd Higgs state and the average squark mass, respectively; the loop function  $h_2(x_{\tilde{g}})$  can be found in the app. A of [50] while

$$\epsilon_{\tilde{g}} \simeq \frac{2\alpha_3}{3\pi} \frac{\mu m_{\tilde{g}}}{\tilde{m}^2} \left( \frac{1}{1 - x_{\tilde{g}}} + \frac{x_{\tilde{g}}}{(1 - x_{\tilde{g}})^2} \log x_{\tilde{g}} \right). \quad (20)$$

The neutral Higgs contribution becomes important and hence competitive with the gluino box contribution for  $\tan\beta \gtrsim 30 - 50$ . For  $\tan\beta \lesssim 20$  it is negligible compared to that of the gluino box.

The  $K_L - K_S$  mass difference and the CP-violating parameter of the kaon system are then calculated by

$$\Delta m_K = 2\Re\langle K^0 | \mathcal{H}_{\text{eff}} | \bar{K}^0 \rangle, \quad (21)$$

$$\epsilon_K = \frac{1}{\sqrt{2}\Delta m_K} \Im\langle K^0 | \mathcal{H}_{\text{eff}} | \bar{K}^0 \rangle. \quad (22)$$

---

<sup>3</sup>Strictly speaking there are three different values of the Higgsing scale:  $m_{v_k}^2 = 2(g_{A_k}^2 + g_{B_k}^2)v^2$ , but when we omit the index  $k$ , a geometric average value of the three scales is understood.

The matrix elements can be found in [51–53] and recent results for the bag parameters in [54, 55], while the RG evolution of the matrix elements is done using the magic numbers of [52].

The mass insertions are given by the off-diagonal elements of the (here down-type) squark mass-squared matrix in the super-CKM basis [56] divided by the average squark mass-squared

$$(\delta_d^{MN})_{ij} = \frac{(\mathcal{M}_{\tilde{d}}^{MN})_{ij}^2}{\tilde{m}^2} = \frac{\left( V_M^d \text{diag}(m_{\tilde{d},M}^2, m_{\tilde{s},M}^2, m_{\tilde{b},M}^2) (V_N^d)^\dagger \right)_{ij} \delta^{MN}}{\tilde{m}^2}, \quad (23)$$

where  $M, N = L, R$ , and  $i, j = 1, 2, 3$ . We are neglecting the  $LR, RL$  elements due to vanishing  $A$ -terms. The matrices  $V_{M,N}^d$  are the bi-unitary rotation matrices used to diagonalize the down-type fermions. Since we work with the two-nodes model of fig. 1, the first two generations of squarks are mass-degenerate at the messenger scale  $M$ . Defining  $\Delta m_d^2 \equiv m_b^2 - m_d^2 = m_b^2 - m_s^2$ , we can write

$$(\delta_d^{MM})_{ij} = (\eta_d^{MM})_{ij} \frac{\Delta m_d^2}{\tilde{m}^2}, \quad (\eta_d^{MM})_{ij} \equiv (V_M^d)_{i3} (V_M^{d\dagger})_{3j}, \quad (24)$$

where  $(\eta_d^{MM})_{ij} \leq 1/2$  are matrix elements that depend on the basis of the Yukawa matrices. The reason why the coefficients are smaller than  $1/2$  is geometric. Let us consider an  $SU(2)$  subgroup, for which we can write e.g. the element

$$|(\eta_d^{MM})_{13}| = \sqrt{x(1-x)} \leq \frac{1}{2}, \quad [0, 1] \ni x = (n_1^2 + n_2^2) \sin^2 \alpha, \quad (25)$$

where  $n_{1,2,3}$  is a (real) three-component unit vector and  $\alpha \in \mathbb{R}$  is a real number. We would like to present a conservative flavor analysis, i.e. not assuming any alignments or tuning of complex phases. The most conservative choice would thus be to set  $(\eta_d^{MM})_{13,23} = 1/2$ . However, in order to see if such a choice is by any means realistic in the model at hand, we perform a Monte Carlo analysis, presented in app. B. It is done setting  $\tan \beta = 20$  and assuming the Yukawa texture (2) with coefficients in the range  $0.1 - 2$ . All the random matrices generated have coefficients producing the measured quark (lepton) masses as well as the best-fit CKM matrix. For each such generated Yukawa matrix, we calculate the diagonalization matrices which by eq. (24) gives us  $(\eta_{u,d}^{MM})_{ij}$ . The analysis shows that in the squark sector the largest values of  $(\eta_d^{MM})_{13,23}$  are about  $\sim 1/4$  and  $\sim 1/2$  in the slepton sector. Notice that the specific choice of texture,  $\tan \beta$  and the coefficients are such that the  $(\eta_d^{RR})_{13,23} \lesssim 0.08$ . We will not incorporate this into the presented flavor constraints, as it depends on choices made in the Monte Carlo, but we will use this information in the summary plots presented in the end of this section.

That is, we would like the analysis to represent the generic constraints for the model, also if we change  $\tan \beta$  or the link field representation [9]. Due to above discussion, we choose to present the flavor constraints with

$$(\eta_u^{MM})_{13,23} = \frac{1}{4}, \quad (\eta_d^{MM})_{13,23} = \frac{1}{4}, \quad (\eta_\ell^{MM})_{13,23} = \frac{1}{2}, \quad (\eta_e^{MM})_{13,23} = \frac{1}{2}. \quad (26)$$

The second ingredient in the  $\delta s$  is the actual mass-splitting, which is intrinsic and is generated at the messenger scale  $M$  due to the fact that the model is a two-nodes model (see fig. 1). The mass-splitting generated at the messenger scale is calculated exactly in app. A. The exact expressions are given by eq. (48) with the form factors in app. A.3, while an expansion to second order in  $1/y$  is given by eq. (58). Using eq. (58), we find the mass splitting at the messenger scale

$$\frac{\Delta m_{L,R}^2}{\tilde{m}^2} \sim \pm c \times \frac{2\lambda_{\text{av}}^{LL,RR} \log^2 y^2}{y^2}, \quad \lambda_{\text{av}}^{LL} \equiv \frac{1}{3} \sum_{k=1}^3 \frac{g_B^2}{g_{\text{eff},k}^2}, \quad \lambda_{\text{av}}^{RR} \equiv \frac{1}{2} \sum_{k=1,3} \frac{g_B^2}{g_{\text{eff},k}^2}, \quad (27)$$

where  $+$  ( $-$ ) is for the normal (inverted) model and  $c$  is an order one constant determined by the messenger sector matrix  $\mathcal{M}$  while  $y \equiv m_v/M$ . In the case of the high-scale mediation model of sec. 3,  $c \sim 1$  will be a function of  $\alpha$  but having only a mild dependence for  $\alpha \lesssim 1$  in the relevant parameter space.

The contribution to the  $\delta$ s described so far is the intrinsic one due to the mass splitting at the messenger scale. RG evolution [57] will also induce a contribution to the  $\delta$ s which can be split into a MFV (minimal flavor violation) and a non-MFV part

$$\begin{aligned}
(\delta_u^{LL})_{i3}^{\text{RG}} &\sim \frac{t}{8\pi^2} \left( 2 + \frac{m_{H_d}^2}{\tilde{m}^2} \right) |Y_b|^2 K_{i3}^\dagger K_{33} + \frac{t}{16\pi^2} \frac{\Delta m_L^2}{\tilde{m}^2} \left[ |Y_t|^2 (\eta_u^{LL})_{i3} + |Y_b|^2 (\eta_u^{LL})_{ik} K_{k3}^\dagger K_{33} \right. \\
&\quad \left. + |Y_b|^2 K_{i3}^\dagger K_{3k} (\eta_u^{LL})_{k3} + 2|Y_b|^2 \frac{\Delta m_R^2}{\Delta m_L^2} K_{i3}^\dagger (\eta_d^{RR})_{33} K_{33} \right], \tag{28}
\end{aligned}$$

$$(\delta_u^{RR})_{i3}^{\text{RG}} \sim \frac{t}{8\pi^2} \frac{\Delta m_R^2}{\tilde{m}^2} |Y_t|^2 (\eta_u^{RR})_{i3}, \tag{29}$$

$$\begin{aligned}
(\delta_d^{LL})_{i3}^{\text{RG}} &\sim \frac{t}{8\pi^2} \left( 2 + \frac{m_{H_u}^2}{\tilde{m}^2} \right) |Y_t|^2 K_{i3} K_{33}^\dagger + \frac{t}{16\pi^2} \frac{\Delta m_L^2}{\tilde{m}^2} \left[ |Y_b|^2 (\eta_d^{LL})_{i3} + |Y_t|^2 (\eta_d^{LL})_{ik} K_{k3} K_{33}^\dagger \right. \\
&\quad \left. + |Y_t|^2 K_{i3} K_{3k}^\dagger (\eta_d^{LL})_{k3} + 2|y_t|^2 \frac{\Delta m_R^2}{\Delta m_L^2} K_{i3} (\eta_u^{RR})_{33} K_{33}^\dagger \right], \tag{30}
\end{aligned}$$

$$(\delta_d^{RR})_{i3} \sim \frac{t}{8\pi^2} \frac{\Delta m_R^2}{\tilde{m}^2} |Y_b|^2 (\eta_d^{RR})_{i3}, \tag{31}$$

$$(\delta_\ell^{LL})_{i3} \sim \frac{t}{8\pi^2} \frac{\Delta m_{\ell,L}^2}{\tilde{m}_\ell^2} |Y_\tau|^2 (\eta_\ell^{LL})_{i3}, \tag{32}$$

$$(\delta_e^{RR})_{i3} \sim \frac{t}{8\pi^2} \frac{\Delta m_{e,R}^2}{\tilde{m}_\ell^2} |Y_\tau|^2 (\eta_e^{RR})_{i3}, \tag{33}$$

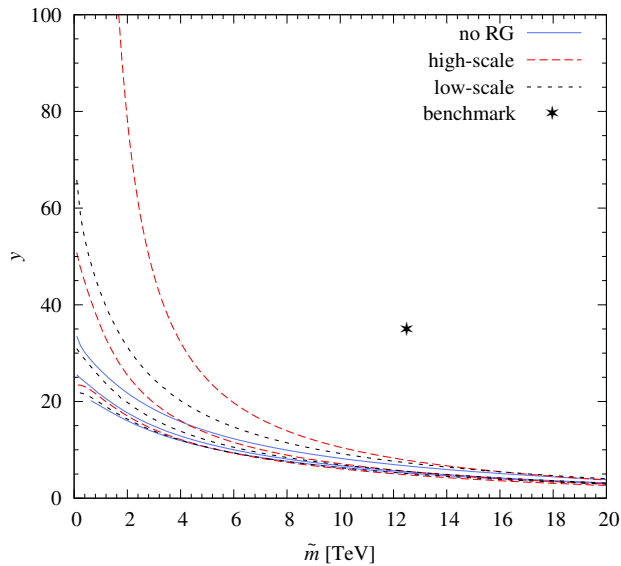
where  $i = 1, 2$ ,  $t = \log(m_t/M)$  is the range of the RG running and  $K^T$  is the CKM matrix. The first terms in eqs. (28) and (30) are of MFV type while all the other terms are not, but are proportional to the intrinsic mass splitting  $\Delta m^2$  due to the model being a two-nodes quiver, generated at the messenger scale.

Now we are ready to present the flavor constraints for the models at hand. In fig. 7 we show the results of the constraints due to  $K - \bar{K}$  mixing coming from both gluino box diagrams at fourth order in the MI approximation, i.e. two MIs with double flavor-flip ( $2 \rightarrow 3$  and  $3 \rightarrow 1$ ) in the super-CKM basis (recall that the flavor changing  $2 \rightarrow 1$  process is negligible as the first two generations are degenerate at the messenger scale). We have set the gluino mass to be 1150 GeV for all the constraints. The experimental limits used are summarized in tab. 2. The benchmark point shown in fig. 2 is indicated in all the flavor constraints with a black star.

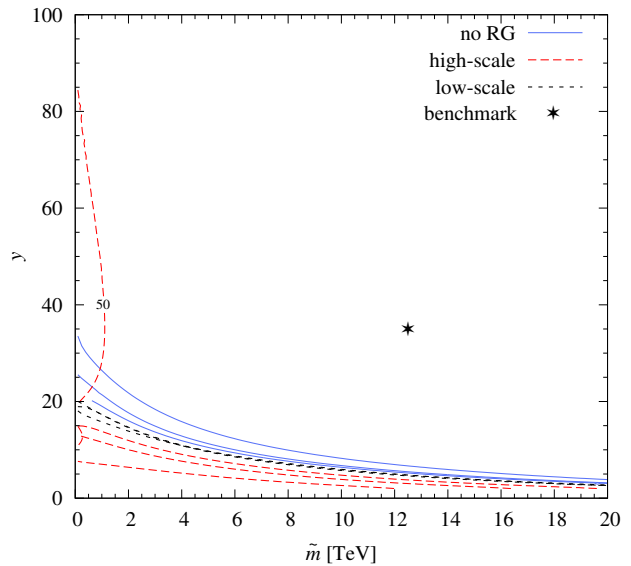
Using the same diagrams, i.e. gluino boxes and Higgs penguins, we calculate the constraints on the CP-violating parameter  $\epsilon_K$  which are shown in fig. 8. For the plots,  $\Delta m_K$  is set to the experimental bound, and we assume order one complex phases in the matrix elements, hence this is a conservative estimate. Notice that in the model at hand, we have potentially two complex phases that cannot be set to zero [9] and hence can induce CP-violating effects as measured by  $\epsilon_K$  (as well as the EDMs to be discussed shortly).

In the case of  $B_d - \bar{B}_d$ , the dominant Wilson coefficients are given by single flavor-flipped second order MIs, see [50], and the magic numbers and matrix elements can be found in [62]. Even though the boxes are only at second order in the MI expansion, the  $B_q - \bar{B}_q$  contributions are only comparable to the  $K - \bar{K}$  ones (even though at fourth order in MI). By explicit calculations we find that the  $B_d - \bar{B}_d$  constraints are down with respect to the  $K - \bar{K}$  ones by about a factor of two (the  $B_s - \bar{B}_s$  are even more subdominant).





(a) Two-node quiver



(b) Inverted two-node quiver

Figure 7: Constraints on  $\Delta m_K$  from gluino box diagrams and double Higgs penguin diagrams in the  $(\tilde{m}, y)$ -plane for a) the normal and b) the inverted quiver model. The three lines (from above) represent  $\tan \beta = 50, 30, 10$ . The gluino mass is set to  $1150 \text{ GeV}$ ,  $\mu = \tilde{m}/2$  and  $m_H = 2\tilde{m}/3$ . The Higgs contributions kick in at  $\tan \beta \gtrsim 30$ . The relation between the average squark mass,  $\tilde{m}$ , and  $\tan \beta$  is sensitive to the properties of the messenger sector (e.g. the values of  $M, \alpha, z$ ) as well as the precise value of the SM parameters (e.g. a slight change of  $m_t, m_h$  and  $\alpha_3$  feeds large modifications to  $\tilde{m}$  via RG evolution); this and the following figures thus span the full relevant parameter space.

Observable	Limit
$\Delta m_K$	$3.484 \times 10^{-15}$ GeV [37]
$\Delta m_D$	$1.30 \times 10^{-14}$ GeV [58]
$\Delta m_{B_d}$	$3.337 \times 10^{-13}$ GeV [37]
$ \epsilon_K $	$2.228 \times 10^{-3}$ [37]
$\text{Br}(\mu \rightarrow e\gamma)$	$5.7 \times 10^{-13}$ [59]
$ d_e $	$1.05 \times 10^{-27}$ e cm (90% CL.) [60]
$ d_n $	$2.9 \times 10^{-26}$ e cm (90% CL.) [61]

Table 2: Experimental limits used in the presented plots.

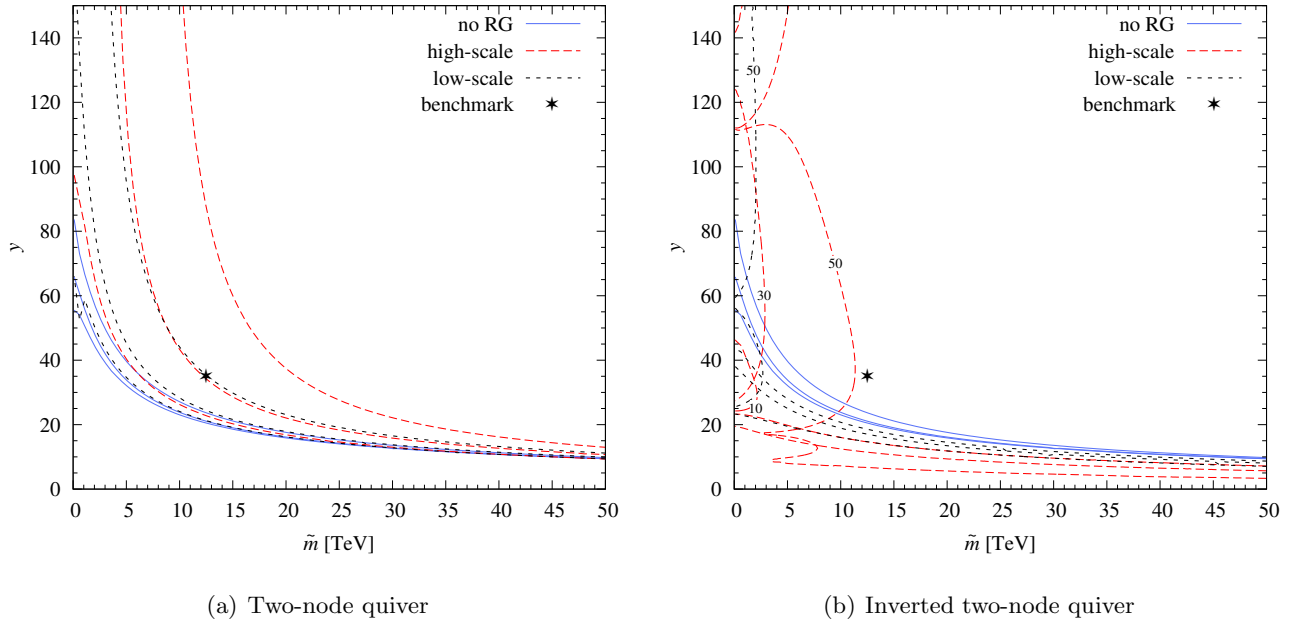


Figure 8: Constraints on  $|\epsilon_K|$  from gluino box diagrams as well as double Higgs penguin diagrams in the  $(\tilde{m}, y)$ -plane. The three lines (from above) represent  $\tan \beta = 50, 30, 10$ . The gluino mass is set to 1150 GeV,  $\mu = \tilde{m}/2$  and  $m_H = 2\tilde{m}/3$ . The Higgs contributions kick in at  $\tan \beta \gtrsim 30$ .

We have also checked the  $D - \bar{D}$  mixing which like in the kaon case needs the double flavor-flipped MI to kick in (the Wilson coefficients are given by eq. (18) with  $\delta_d \rightarrow \delta_u$ ). The matrix elements, bag parameters and magic numbers are given in [63]. Due to the experimental limits (see tab. 2), these constraints are less severe than the kaon ones. We find that due to the RG effects on the mass-splitting – because of the large top-Yukawa – the  $D - \bar{D}$  meson mixing constraint is of the same order as the  $B_d - \bar{B}_d$  constraint; both about a factor of two less important than the kaon ones. The  $B_d - \bar{B}_d$  constraints are stronger than the  $D - \bar{D}$  ones for the average squark mass less than about 6 TeV, which however is not possible in the model and part of parameter space that we are investigating here.

The next flavor observables we check are  $\Delta F = 1$  processes. We find that the most important one is due to the gaugino and slepton mediated decay,  $\mu \rightarrow e\gamma$ . The important amplitude again has a double

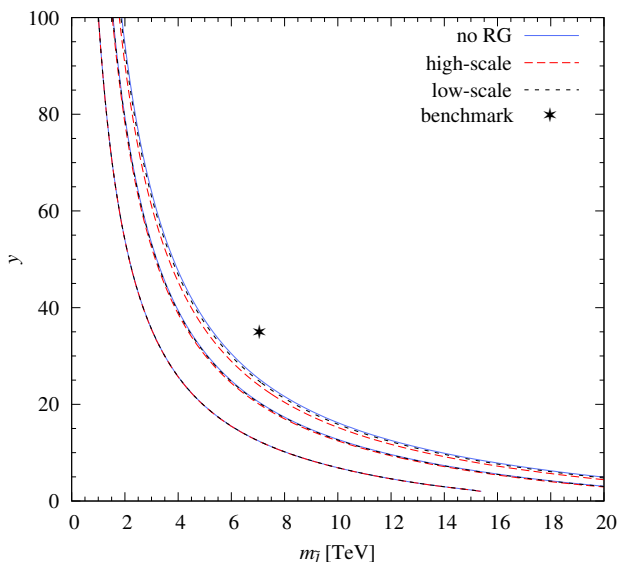


Figure 9: Constraints on  $\text{Br}(\mu \rightarrow e\gamma)$  from gaugino and slepton mediated decay in the  $(m_{\tilde{\ell}}, y)$ -plane, where  $m_{\tilde{\ell}}$  is the average slepton mass. The three lines (from above) represent  $\tan\beta = 50, 30, 10$ . We took  $\mu = m_{\tilde{\ell}}$  and  $M_1 = 192$  GeV. The constraints are equal for the normal and the inverted model.

flavor-flipped MI and reads [64, 50]

$$A_{L,R}^{21} \simeq \frac{\alpha_1 m_\tau \mu M_1 \tan\beta}{4\pi m_\mu m_\ell^4} (\delta_e^{RR})_{23} (\delta_\ell^{LL})_{31} f_{4n}(x_1), \quad (34)$$

where  $m_\tau$ ,  $m_\mu$ ,  $\mu$ ,  $M_1$  and  $m_{\tilde{\ell}}$  are the tau mass, the muon mass, the supersymmetric Higgs mass, the bino mass and the average slepton mass, respectively.  $x_1 \equiv M_1^2/m_{\tilde{\ell}}^2$ . The loop function  $f_{4n}(x_1)$  can be found in app. A of [50]. This amplitude is especially important due to an enhancement factor of  $m_\tau/m_\mu$  with respect to that of [65, 48].<sup>4</sup> The branching ratio can then be expressed as

$$\frac{\text{BR}(\mu \rightarrow e\gamma)}{\text{BR}(\mu \rightarrow e\nu_\mu\bar{\nu}_e)} = \frac{48\pi^3\alpha}{G_F^2} (|A_L^{21}|^2 + |A_R^{21}|^2). \quad (35)$$

The constraints are shown in fig. 9. Let us mention that the MEG corporation plans a possible upgrade which could increase the experimental limit by one order of magnitude [66], potentially probing very far with this flavor observable; see also [67, 68].

We checked also other  $\Delta F = 1$  processes such as the gluino mediated contribution to  $b \rightarrow s\gamma$  (the charged Higgses are too heavy in our model to be of any importance [69]) as well as the Higgs mediated penguin contributions to  $B_s \rightarrow \mu^+\mu^-$  [50]. These constraints were subdominant with respect to the above discussed processes.

The next checks we perform are on the electric dipole moments (EDMs). Although they typically are classified as  $\Delta F = 0$  observables, the dominant ones that we check here are of the so-called “flavored”

<sup>4</sup>Note that the Monte Carlo analysis of app. B finds relatively large maximum values for  $(\delta_\ell^{RR})_{12}$  which could potentially be important. We checked however the single MI contribution and it is much less important than the double MI contribution discussed here.

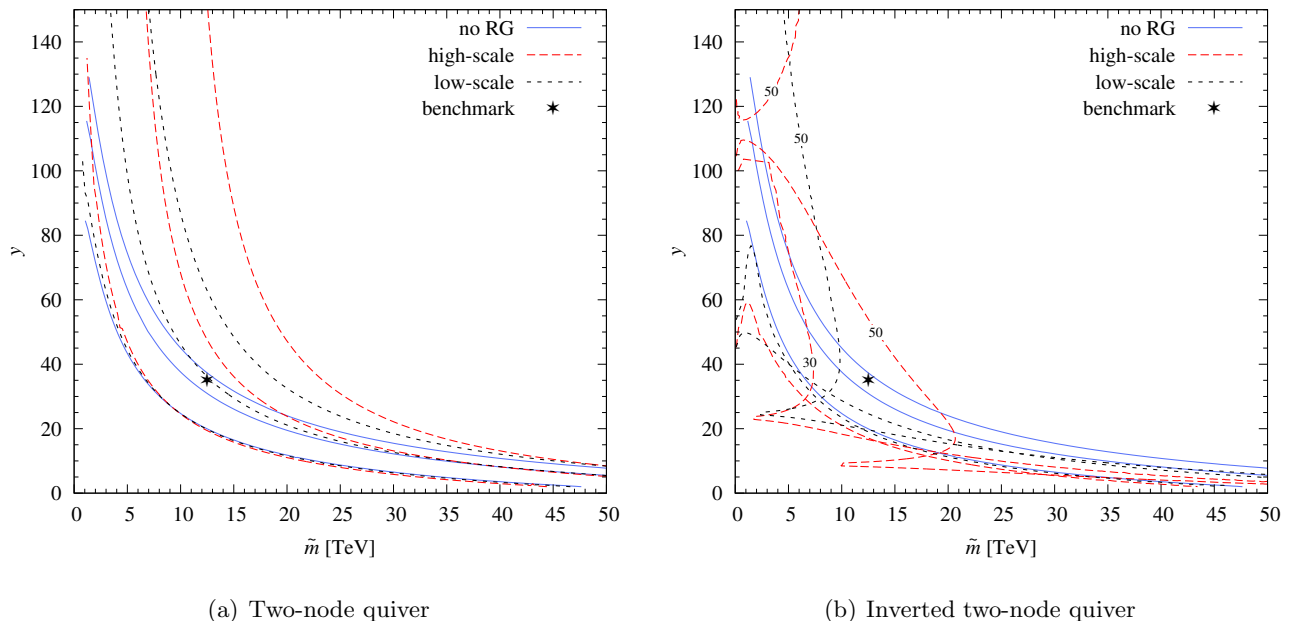


Figure 10: Constraints on  $|d_n|$  from gluino/squark diagrams in the  $(\tilde{m}, y)$ -plane. The three lines (from above) represent  $\tan\beta = 50, 30, 10$ . We took  $\mu = \tilde{m}/2$  and  $m_{\tilde{g}} = 1150$  GeV.

type, i.e. they consist of two  $\Delta F = 1$  transitions. Since we do not have sizable  $A$ -terms, the dominant contribution is to the down-quark chromo-EDM and reads [70, 50]

$$\{d_d/e, d_d^c\} \simeq -\frac{\alpha_3}{4\pi} \frac{m_b}{\tilde{m}^2} \frac{m_{\tilde{g}}\mu}{\tilde{m}^2} \frac{\tan\beta}{1 + \epsilon_{\tilde{g}} \tan\beta} \Im [(\delta_d^{LL})_{13}(\delta_d^{RR})_{31}] f_{\tilde{g}}^d(x_{\tilde{g}}), \quad (36)$$

where the loop functions can be found in app. A of [50]. Although the quark EDMs have not been measured, they are related to that of the neutron by a QCD sum rule estimate [71]

$$d_n = (1 \pm 0.5) [1.4(d_d - 0.25d_u) + 1.1e(d_d^c + 0.5d_u^c)], \quad (37)$$

which is limited by experiments on ultra-cold neutrons, see tab. 2. As mentioned, we have two complex phases that we cannot eliminate and that can be of order one. Here we assume order one phases, although accidentally smaller phases would reduce the present constraints. The constraints we find are shown in fig. 10.

We also check the EDM of the electron which has the leading contribution at double flavor-flipped MI (second order) [72, 50]

$$\frac{d_e}{e} \simeq \frac{\alpha_1}{4\pi} \frac{M_1}{m_{\tilde{\ell}}^2} \frac{m_\tau \tan\beta}{m_{\tilde{\ell}}^2} \Im [\mu(\delta_{\ell}^{LL})_{13}(\delta_e^{RR})_{31}] f_{4n}(x_1). \quad (38)$$

The constraints are displayed in fig. 11. Experimentally, the limit comes from measuring Ytterbium-Fluoride (YbF) and is given in tab. 2. Future EDM measurements could conceivably push up the limit by almost two orders of magnitude [73], which could make this flavor observable one of the tightest.

A comment in store is due to the conservative choice of setting  $(\eta_{u,d}^{MM})_{13,23} = 1/4$  and  $(\eta_{\ell,e}^{MM})_{13,23} = 1/2$  (see eq. (24)) in the shown flavor constraints. This is the worst-case scenario for the model at hand. This

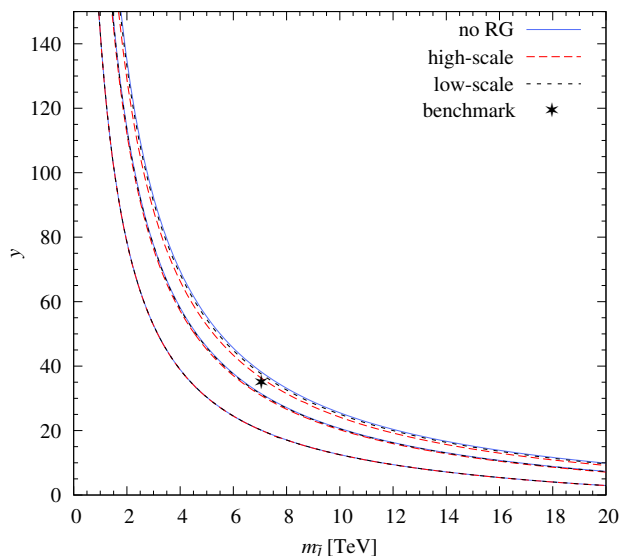


Figure 11: Constraints on  $|d_e|$  from gluino/squark diagrams in the  $(m_{\tilde{\ell}}, y)$ -plane, with  $m_{\tilde{\ell}}$  being the average slepton mass. The three lines (from above) represent  $\tan\beta = 50, 30, 10$ . We took  $\mu = m_{\tilde{\ell}}$  and  $M_1 = 192$  GeV. The constraints are equal for the normal and the inverted model.

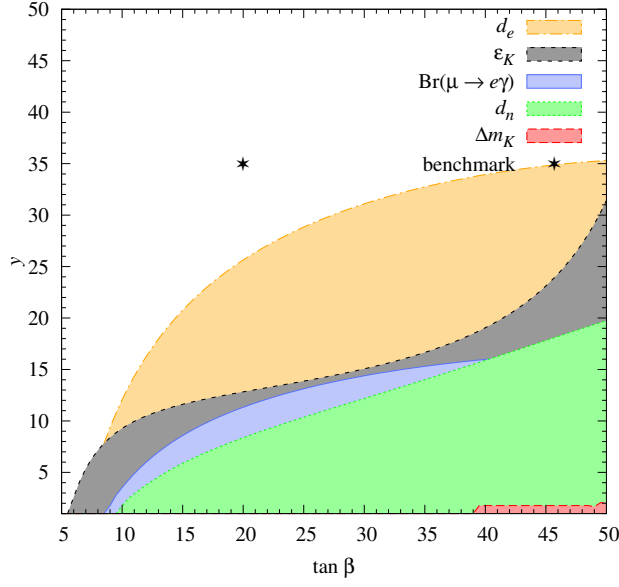
Constraint	Scaling formula	$\max(\eta)$	$\sqrt{\langle\eta^2\rangle}$
$\Delta m_K,  \epsilon_K  (C_4)$	$\tilde{m} \rightarrow 16\sqrt{(\eta_d^{LL})_{23}(\eta_d^{LL})_{31}(\eta_d^{RR})_{23}(\eta_d^{RR})_{31}} \tilde{m}$	$\tilde{m} \rightarrow 0.29\tilde{m}$	$\tilde{m} \rightarrow 0.081\tilde{m}$
$\Delta m_D$	$\tilde{m} \rightarrow 16\sqrt{(\eta_u^{LL})_{23}(\eta_u^{LL})_{31}(\eta_u^{RR})_{23}(\eta_u^{RR})_{31}} \tilde{m}$	$\tilde{m} \rightarrow 0.71\tilde{m}$	$\tilde{m} \rightarrow 0.20\tilde{m}$
$ d_n $	$\tilde{m} \rightarrow (16(\eta_d^{LL})_{13}(\eta_d^{RR})_{31})^{1/3} \tilde{m}$	$\tilde{m} \rightarrow 0.66\tilde{m}$	$\tilde{m} \rightarrow 0.43\tilde{m}$
$\text{Br}(\mu \rightarrow e\gamma)$	$m_{\tilde{\ell}} \rightarrow (8(\eta_{\ell}^{LL})_{31}^2(\eta_e^{RR})_{23}^2 + 8(\eta_{\ell}^{RR})_{31}^2(\eta_e^{LL})_{23}^2)^{1/6} m_{\tilde{\ell}}$	$m_{\tilde{\ell}} \rightarrow 0.77m_{\tilde{\ell}}$	$m_{\tilde{\ell}} \rightarrow 0.48m_{\tilde{\ell}}$
$ d_e $	$m_{\tilde{\ell}} \rightarrow (4(\eta_{\ell}^{LL})_{13}(\eta_e^{RR})_{31})^{1/3} m_{\tilde{\ell}}$	$m_{\tilde{\ell}} \rightarrow 0.77m_{\tilde{\ell}}$	$m_{\tilde{\ell}} \rightarrow 0.48m_{\tilde{\ell}}$

Table 3: Scaling of the average mass in the presented graphs for fixed  $y$ .  $\eta$  in the 3rd and 4th column refers to the value of the elements of eq. (24) which are estimated by the Monte Carlo method in app. B.

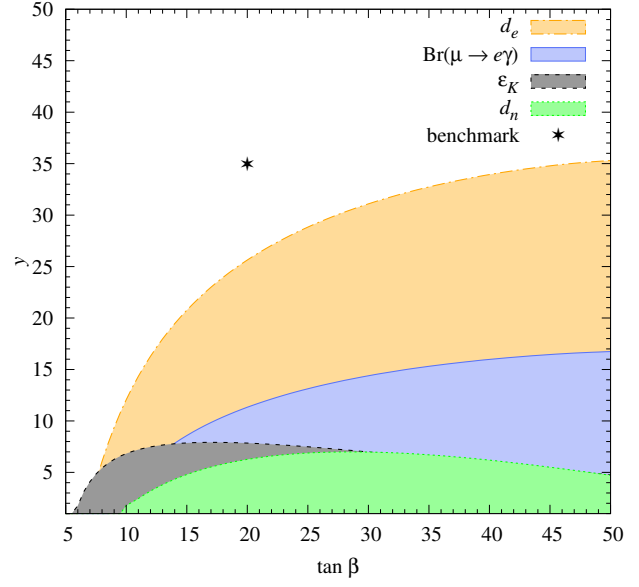
conservative value is chosen as to display the farthest possible sensitivity for the respective constraint. If the  $\eta$ s are changed by a factor of order one, we can crudely ignore the loop factor and thus for fixed  $y$  on the graphs, the  $x$ -axis is simply rescaled by a power law, see tab. 3.

Finally, we also checked whether the model is able to produce a measured discrepancy [74] between the SM prediction and the current measurements of the  $(g-2)_\mu$  using the formulae of [75]. However, due to the heavy sleptons and large value of  $\mu$ , the SUSY contribution is typically two orders of magnitude too small to explain the  $3\sigma$  anomaly [76].

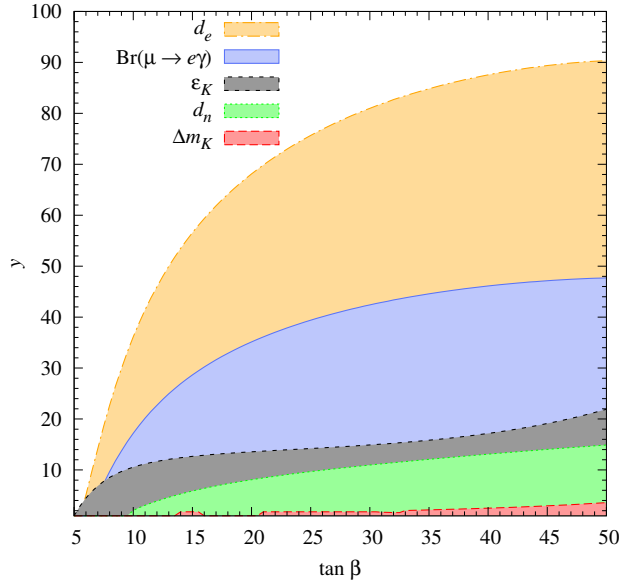
To recapitulate, we present a summary plot for both the high-scale and the low-scale models in fig. 12, using the maximal values of the  $\eta$ s from the Monte Carlo analysis of app. B.



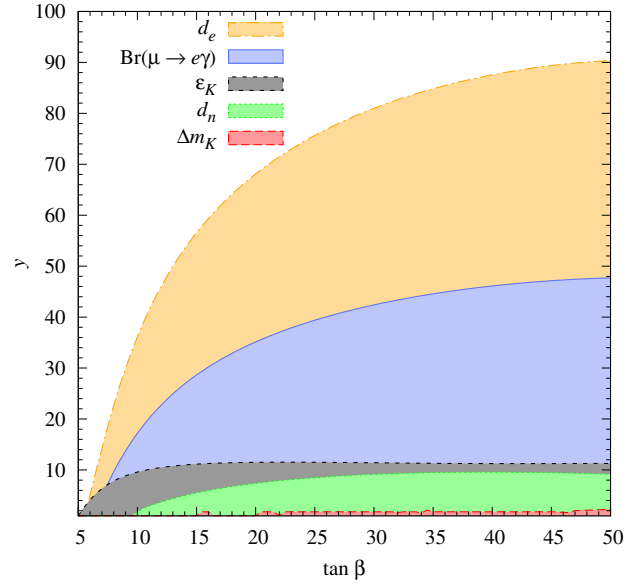
(a) High-scale – two-node quiver



(b) High-scale – inverted two-node quiver



(c) Low-scale – two-node quiver



(d) Low-scale – inverted two-node quiver

Figure 12: Summary of all the presented flavor constraints in the  $(\tan \beta, y)$ -plane. The  $\eta$ s have been set to their maximal values according to the Monte Carlo analysis of app. B, see tab. 4. We have set  $M_1 = 192$  GeV and  $m_{\tilde{g}} = 1150$  GeV. Notice that the constraints shown are sensitive to the model point (and thus the messenger sector). Note also that the average squark mass,  $\tilde{m}$ , is calculated for each value of  $\tan \beta$  using the face-values of the SM parameters,  $m_t, m_h$  and  $\alpha_3$ ; this plot is therefore sensitive to variations of the latter parameters as well as of the  $\eta$ s.

## 7 Dark matter

### 7.1 High-scale mediation case

In the high-scale mediation case there are two possibilities, either the gravitino or the mostly-bino neutralino is the LSP and can potentially make it as a dark matter candidate. For sizable  $\tan\beta \gtrsim 6$  the gravitino is the LSP with the bino being the NLSP, while for  $\tan\beta \lesssim 6$  the bino becomes the LSP with the gravitino the NLSP.

The corner where the neutralino becomes the LSP – i.e. when  $\tan\beta \lesssim 6$  – is not a favorable situation for dark matter as the  $\mu$ -term rises sharply into the multi-TeV regime, see fig. 4. Hence the neutralino which is almost purely bino has a mass  $\sim 160$  GeV  $\ll \mu \sim 35 - 50$  TeV and therefore the bino is nearly decoupled and annihilates too weakly in the early Universe [12].

For most values of  $\tan\beta$ , the gravitino is the LSP and since we are working in a gauge-mediated model, it is stable. Due to the reheating temperature being higher than the average squark-mass scale in the model, the dominant production of gravitinos comes from high-energy SUSY scattering processes and the contribution to the present energy density is [77, 13]

$$\Omega_{3/2} h^2 \simeq \left(\frac{\text{GeV}}{m_{3/2}}\right) \left(\frac{m_{\tilde{g}}}{1150 \text{ GeV}}\right)^2 \left(\frac{T_R}{10^{10} \text{ GeV}}\right) \left(\frac{228.75}{g_*(T_R)}\right)^{3/2} 26.5. \quad (39)$$

Using the recent Planck result,  $\Omega_{\text{DM}} h^2 = 0.1186 \pm 0.0031$  (including lensing) [78] which is a larger amount of dark matter compared to results for instance from WMAP, we obtain an upper bound (from overclosure of the Universe) and a lower bound (from contributing all the dark matter of the Planck result) on the reheating temperature

$$1.2 \times 10^9 \text{ GeV} \lesssim T_R \lesssim 1.3 \times 10^9 \text{ GeV}, \quad (40)$$

for a 28 GeV gravitino in the  $1\sigma$  window of the Planck measurement or less if the gravitinos do not make up all the observed dark matter. This reheating temperature is just near the lower bound for a successful thermal leptogenesis [79–81]. For big bang nucleosynthesis (BBN) much lower reheating temperatures are allowed.

A more severe constraint is due to the bino decaying into gravitinos and photons, where the photons are potentially damaging, depending on the life time of the bino, which reads [13]

$$\tau_{\chi_1^0} \simeq \left(\frac{m_{3/2}}{\text{GeV}}\right)^2 \left(\frac{\text{GeV}}{m_{\chi_1^0}}\right)^5 6 \times 10^{14} \text{ sec}. \quad (41)$$

For the life time of the bino in the range  $10^2 - 10^7$  sec (hadron decays) and  $10^7 - 10^{10}$  sec (electromagnetic decays), there are constraints due to the photo destruction of light nuclei that are synthesized during BBN [82, 18, 83]. For the life time in the range  $10^{10} - 10^{13}$  sec, there are constraints from spectral distortions of the cosmic microwave background radiation [84–87]. Finally, for the life time in the range  $10^{13} - 10^{18}$  sec, diffuse gamma-ray observations put limits on the decays [88]. Life times even longer yield practically stable NLSPs, which means that the only constraint is due to the total energy density of the dark matter.

The life time given in eq. (41) for a 28 GeV gravitino and 192 GeV bino yields  $\tau_{\chi_1^0} \sim 1.8 \times 10^6$  sec, which is in conflict with the above mentioned bounds from BBN [89, 83]<sup>5</sup>. This kind of analysis typically makes assumptions about the NLSP yield and that the released energy is of the order of the NLSP mass. Taking a conservative attitude in view of the BBN constraints [89, 83], the life time should be smaller than

---

<sup>5</sup>Notice that assumptions about the bino yield as well as its scaling with the bino mass have been made in the calculation of [83].

roughly 120 sec in order to avoid the overproduction of deuterium or  ${}^4\text{He}$ . This means that for having a stable gravitino, it should either be lighter than  $\sim 230$  MeV (for a 192 GeV bino) or the bino should be heavier than  $\sim 1310$  GeV (for a 28 GeV gravitino). This would lower the reheating temperature by two orders of magnitude and hence rule out the leptogenesis scenario<sup>6</sup>.

There are several ways to modify the properties of the benchmark points chosen here, to allow viable gravitino DM within our class of models, e.g.:

- The simplest way, suggested above, is to lower the messenger scale  $M$  and hence the gravitino mass  $m_{3/2}$  so that the conservative bounds from BBN are satisfied. The rest of the spectrum remains almost unaltered.
- One could contemplate the possibility that  $k \equiv F/F_0 = \mathcal{O}(10^{-1})$ , which would make the gravitino of the benchmark point of fig. 2 as heavy as the bino. In the case that it is nearly degenerate (the possibility of the nearly degenerate NLSP gravitino and LSP neutralino is also viable), the BBN constraints are drastically weakened [91].

## 7.2 Low-scale mediation case

In the low-scale mediation case, the gravitino is always the LSP and extremely light – of order of keV’s – and hence it would make up warm dark matter whose mass is constrained by the Lyman-alpha forest [92], gamma-ray bursts [93] and galaxy formation [94, 95]. Since in this case the average mass of the superpartners is much larger than that of the gravitino and if so is the reheating temperature, then the gravitinos go in equilibrium giving the density [13]

$$\Omega_{3/2} h^2 \simeq \left( \frac{m_{3/2}}{\text{keV}} \right) \left( \frac{228.75}{g_*} \right) 0.5. \quad (42)$$

If the gravitino mass is 0.237 keV, this yields a warm DM candidate with the observed relic abundance. The question of whether warm DM is a viable candidate is currently being reconsidered, see e.g. [96–98].

Alternatively, in this scenario, one could contemplate the possibility of pseudomoduli DM particles from the secluded sector [99, 100] or the lightest messenger field if a conserved quantum number in the messenger sector is assumed [101]. We will not elaborate on these possibilities here.

## 8 Discussion

In this paper we have studied a mild-split SUSY part of a parameter space present in a class of quiver-like models. The simplest type is a two-nodes quiver model which is able to produce the SM flavor texture, namely, the quark and lepton masses as well as the CKM matrix, and the newly found Higgs mass. In the model as studied in this paper, the Higgs mass is simply fed by top loops up till about 12 TeV, where the stops eventually kick in.

We made a simple one-loop calculation to estimate to which degree the model unifies. Its simplest version matches the measured value of the strong coupling at the  $2 - 3\sigma$  level. There are, however, further effects to consider such as two-loop effects, threshold effects and more importantly, matter from the link sector has not been taken into account. Since the amount of matter in the link field sector is very large, a tiny splitting can modify the unification substantially.

The supersymmetric flavor problem – although simplistically dealt with using near-universality – turns out to be quite near to present flavor constraints, if order one complex phases are taken into account.

---

<sup>6</sup>Note however that some regions of parameter space of e.g. the CMSSM with a gravitino and a bino with the life time in the window of  $10^4 - 10^6$  sec, have been found to be consistent with BBN constraints in [90].



In this model, two such complex phases cannot be set to zero and can be expected to be of order one. Among the important flavor constraints are  $\epsilon_K$ , the branching ratio of  $\mu \rightarrow e\gamma$ , the neutron EDM as well as the electron EDM, at least two of whose limits are expected to be upgraded in the near future.

We have furthermore contemplated the possibility of the gravitino making up the observed dark matter component of the energy balance of the presently observed Universe. There are two possibilities in the model as it stands. In the high-scale mediation case, where standard unification is possible, the gravitino is a cold dark matter component while in the low-scale mediation case, where dynamical embedding is possible, it could plausibly be a warm dark matter component. The cold dark matter component is unlikely to be detected at direct detection experiments and although it does not pose any problems itself, the decays of the NLSP, namely the bino, could make considerable damage to the concordance of cosmology by decaying together with photons that would destroy light nuclei.

We will conclude by tying up loose ends and discussing various differences between the model we have studied in the present paper and other types of split-SUSY models in the literature. The type of split SUSY theories in [11–13, 2] has a different set of ground rules, i.e. the mass scale of the fermions is set by the dark matter and the requirement of unification keeps also the higgsini light by means of e.g. some symmetry. Therefore, in those theories it is possible to have squarks heavy enough for having displaced vertices by means of the longevity of the gluino [11, 102]. In our model, on the other hand, the higgsini and scalar masses are tied together by the nature of gauge mediation, even though we are able to have electroweak scale gaugini. A further restriction is coming from keeping the gluino mass near the present experimental bound while producing electroweak symmetry breaking. Although theoretically conceivable, we have not been able to find numerical spectra for values  $\tan\beta$  less than roughly 5 in our model, due to numerical problems with the precision (the convergence) of the code. In this work, we have focused on the mild-split part of the parameter space, however, for  $\tan\beta$  of order unity, there is possibly a corner with “more split” supersymmetry than what we have studied here. We leave such an option as a future study. In our model for  $\tan\beta \geq 5$ , we have left-handed squarks weighing less than around 140 TeV, which in turn makes the gluino lifetime smaller than about  $6 \times 10^{-18}$  sec for a 1.15 TeV gluino. This is  $\sim 2$  nm and thus not long enough for detecting displaced vertices.

As discussed in more detail in [9], the two-nodes quiver model does in fact only naturally produce the hierarchy between the first two and the third generation fermions. In order to have a naturally generated hierarchy also between the first two generations of fermions, namely, between the up and charm (or down and strange) quarks, a three-nodes quiver can be considered [9]. This requires a sufficiently large VEV of the link field connecting the two nodes hosting the first generations, and requiring this VEV to be below or near the GUT scale can thus further lower the messenger scale  $M$ . This in turn yields a lighter gravitino than in the example we have considered here. The full investigation of such a scenario is out of scope of the present paper, but all the necessary formulae for the sfermion masses are given in app. A upon insertion of the appropriate form factors of [103]. Finally, future investigations could pursue the integration of neutrino masses into the model and estimate what impact it would have on the model with respect to the sflavor constraints.

## Acknowledgments

We thank Roberto Auzzi for discussions. This work is supported in part by the I-CORE Program of the Planning and Budgeting Committee and the Israel Science Foundation (Center No. 1937/12), by the BSF – American-Israel Bi-National Science Foundation, and by a center of excellence supported by the Israel Science Foundation (grant number 1665/10).

## A Sfermion masses

In this section, we provide two-loop formulae for the soft masses for a field in an arbitrary representation of any gauge group of a generic quiver-like model with a general messenger sector. The mass formula is used to calculate the mass-splitting in the two-nodes model at the messenger scale, which is the essential ingredient in the flavor analysis presented in sec. 6.

### A.1 Generic messenger sector in a generic quiver

Let us consider a generic messenger sector following [36] given by

$$\int d^4\theta \left[ T_i^\dagger (\delta_{ij} + V\tilde{\lambda}_{ij}) T_j + \tilde{T}_i^\dagger (\delta_{ij} + V\tilde{\lambda}_{ij}) \tilde{T}_j \right] + \int d^2\theta \tilde{T}_i \tilde{\mathcal{M}}_{ij} T_j + \text{c.c.}, \quad (43)$$

where  $i, j = 1, \dots, 2p$  with  $p$  a non-negative integer specifying the number of copies of two-by-two messenger matrices. Now, passing to a basis where the fermionic messengers have a diagonal and real mass matrix  $m_i$ , the complex scalars have, by means of a unitary transformation, the mass-squared matrix

$$\tilde{\mathcal{M}}_\pm = \mathbf{1}_p \otimes (m \pm F\lambda - D\tilde{\lambda}), \quad (44)$$

whose unitary diagonalization matrices are needed in the calculation of the soft masses and are denoted by  $U_\pm^\dagger \tilde{\mathcal{M}}_\pm U_\pm = \text{diag}(m_{\pm 1}^2, \dots, m_{\pm 2p}^2)$ . The gaugino masses are unaltered compared to [36] and the sfermion masses are given by

$$m_{\tilde{f}}^2 = 2 \sum_{k=1}^3 \left( \frac{\alpha_k}{4\pi} \right)^2 C_{\tilde{f},k} n_k \mathcal{E}[f_k(p^2)], \quad (45)$$

where the mass function is defined as

$$\begin{aligned} \mathcal{E}[f(p^2)] \equiv & \int \frac{d^4p d^4q}{\pi^4} f(p^2) \left[ -\frac{1}{4} \sum_{\pm, i, j} (U_\pm^\dagger U_\mp)_{ij} (U_\mp^\dagger U_\pm)_{ji} \frac{1}{p^2[q^2 + m_{\mp j}^2][(p+q)^2 + m_{\pm i}^2]} \right. \\ & + \sum_{\pm, i, j} (U_\pm^\dagger)_{ij} (U_\pm)_{ji} \frac{p^2 + m_{\pm i}^2 - m_j^2}{p^4[q^2 + m_j^2][(p+q)^2 + m_{\pm i}^2]} \\ & \left. - \sum_{\pm, i} \frac{\frac{1}{4}p^2 + m_{\pm i}^2}{p^4[q^2 + m_{\pm i}^2][(p+q)^2 + m_{\pm i}^2]} - \sum_i \frac{p^2 - 2m_i^2}{p^4[q^2 + m_i^2][(p+q)^2 + m_i^2]} \right]. \end{aligned} \quad (46)$$

Using the method of [103], we can calculate the integrals for an arbitrary quiver theory in terms of the following coefficients

$$\begin{aligned} \frac{f(p^2)}{p^2} &= \frac{a_0}{p^2} + \sum_\ell \frac{a_{1,\ell}}{p^2 + m_\ell^2} + \sum_\ell \frac{a_{2,\ell}}{(p^2 + m_\ell^2)^2}, \\ \frac{f(p^2)}{p^4} &= \frac{b_{-1}}{p^2} + \frac{b_0}{p^4} + \sum_\ell \frac{b_{1,\ell}}{p^2 + m_\ell^2} + \sum_\ell \frac{b_{2,\ell}}{(p^2 + m_\ell^2)^2}, \end{aligned} \quad (47)$$

given by the above partial fractions. The result is

$$\begin{aligned}
& \mathcal{E}[f(p^2)] \\
&= \sum_{\pm, i, j} (U_{\pm}^{\dagger} U_{\mp})_{ij} (U_{\mp}^{\dagger} U_{\pm})_{ji} \left( a_0 \alpha_0^a(m_{\mp j}, m_{\pm i}) + \sum_{\ell} a_{1, \ell} \alpha_1^a(m_{\ell}, m_{\mp j}, m_{\pm i}) + \sum_{\ell} a_{2, \ell} \alpha_2^a(m_{\ell}, m_{\mp j}, m_{\pm i}) \right) \\
&+ \sum_{\pm, i, j} (U_{\pm}^{\dagger})_{ij} (U_{\pm})_{ji} \left( a_0 \alpha_0^b(m_j, m_{\pm i}) + \sum_{\ell} a_{1, \ell} \alpha_1^b(m_{\ell}, m_j, m_{\pm i}) + \sum_{\ell} a_{2, \ell} \alpha_2^b(m_{\ell}, m_j, m_{\pm i}) \right. \\
&\quad \left. + b_{-1} \beta_{-1}^b(m_j, m_{\pm i}) + b_0 \beta_0^b(m_j, m_{\pm i}) + \sum_{\ell} b_{1, \ell} \beta_1^b(m_{\ell}, m_j, m_{\pm i}) + \sum_{\ell} b_{2, \ell} \beta_2^b(m_{\ell}, m_j, m_{\pm i}) \right) \\
&+ \sum_{\pm, i} \left( \sum_{\ell} a_{1, \ell} \alpha_1^c(m_{\ell}, m_i, m_{\pm i}) + \sum_{\ell} a_{2, \ell} \alpha_2^c(m_{\ell}, m_i, m_{\pm i}) \right. \\
&\quad \left. + b_{-1} \beta_{-1}^c(m_i, m_{\pm i}) + b_0 \beta_0^c(m_i, m_{\pm i}) + \sum_{\ell} b_{1, \ell} \beta_1^c(m_{\ell}, m_i, m_{\pm i}) + \sum_{\ell} b_{2, \ell} \beta_2^c(m_{\ell}, m_i, m_{\pm i}) \right), \tag{48}
\end{aligned}$$

where the functions are given by

$$\begin{aligned}
\alpha_0^a(m_{\mp j}, m_{\pm i}) &= \frac{1}{2} m_{\pm i}^2 \text{Li}_2 \left( 1 - \frac{m_{\mp j}^2}{m_{\pm i}^2} \right), \tag{49} \\
\alpha_1^a(m_{\ell}, m_{\mp j}, m_{\pm i}) &= \frac{1}{4} m_{\ell}^2 h \left( \frac{m_{\pm i}^2}{m_{\ell}^2}, \frac{m_{\mp j}^2}{m_{\ell}^2} \right) + \frac{1}{2} m_{\pm i}^2 h \left( \frac{m_{\ell}^2}{m_{\pm i}^2}, \frac{m_{\mp j}^2}{m_{\pm i}^2} \right), \\
\alpha_2^a(m_{\ell}, m_{\mp j}, m_{\pm i}) &= -\frac{1}{4} h \left( \frac{m_{\pm i}^2}{m_{\ell}^2}, \frac{m_{\mp j}^2}{m_{\ell}^2} \right), \\
\alpha_0^b(m_j, m_{\pm i}) &= -m_{\pm i}^2 \text{Li}_2 \left( 1 - \frac{m_j^2}{m_{\pm i}^2} \right) - m_j^2 \text{Li}_2 \left( 1 - \frac{m_{\pm i}^2}{m_j^2} \right), \\
\alpha_1^b(m_{\ell}, m_j, m_{\pm i}) &= -m_{\ell}^2 h \left( \frac{m_{\pm i}^2}{m_{\ell}^2}, \frac{m_j^2}{m_{\ell}^2} \right) - m_{\pm i}^2 h \left( \frac{m_{\ell}^2}{m_{\pm i}^2}, \frac{m_j^2}{m_{\pm i}^2} \right) - m_j^2 h \left( \frac{m_{\pm i}^2}{m_j^2}, \frac{m_{\ell}^2}{m_j^2} \right), \\
\alpha_2^b(m_{\ell}, m_j, m_{\pm i}) &= h \left( \frac{m_{\pm i}^2}{m_{\ell}^2}, \frac{m_j^2}{m_{\ell}^2} \right), \\
\alpha_1^c(m_{\ell}, m_i, m_{\pm i}) &= \frac{1}{2} m_{\pm i}^2 h \left( \frac{m_{\ell}^2}{m_{\pm i}^2}, 1 \right) + m_i^2 h \left( \frac{m_{\ell}^2}{m_i^2}, 1 \right) + \frac{1}{4} m_{\ell}^2 h \left( \frac{m_{\pm i}^2}{m_{\ell}^2}, \frac{m_{\pm i}^2}{m_{\ell}^2} \right) + \frac{1}{2} m_{\ell}^2 h \left( \frac{m_i^2}{m_{\ell}^2}, \frac{m_i^2}{m_{\ell}^2} \right), \\
\alpha_2^c(m_{\ell}, m_i, m_{\pm i}) &= -\frac{1}{4} h \left( \frac{m_{\pm i}^2}{m_{\ell}^2}, \frac{m_{\pm i}^2}{m_{\ell}^2} \right) - \frac{1}{2} h \left( \frac{m_i^2}{m_{\ell}^2}, \frac{m_i^2}{m_{\ell}^2} \right),
\end{aligned}$$

$$\beta_{-1}^b(m_j, m_{\pm i}) = -m_j^2(m_{\pm i}^2 - m_j^2)\text{Li}_2\left(1 - \frac{m_{\pm i}^2}{m_j^2}\right) - m_{\pm i}^2(m_{\pm i}^2 - m_j^2)\text{Li}_2\left(1 - \frac{m_j^2}{m_{\pm i}^2}\right), \quad (50)$$

$$\beta_0^b(m_j, m_{\pm i}) = m_j^2\text{Li}_2\left(1 - \frac{m_{\pm i}^2}{m_j^2}\right) - m_{\pm i}^2\text{Li}_2\left(1 - \frac{m_j^2}{m_{\pm i}^2}\right),$$

$$\begin{aligned} \beta_1^b(m_\ell, m_j, m_{\pm i}) &= -m_\ell^2(m_{\pm i}^2 - m_j^2)h\left(\frac{m_{\pm i}^2}{m_\ell^2}, \frac{m_j^2}{m_\ell^2}\right) - m_{\pm i}^2(m_{\pm i}^2 - m_j^2)h\left(\frac{m_j^2}{m_{\pm i}^2}, \frac{m_\ell^2}{m_{\pm i}^2}\right) \\ &\quad - m_j^2(m_{\pm i}^2 - m_j^2)h\left(\frac{m_{\pm i}^2}{m_j^2}, \frac{m_\ell^2}{m_j^2}\right), \end{aligned}$$

$$\beta_2^b(m_\ell, m_j, m_{\pm i}) = (m_{\pm i}^2 - m_j^2)h\left(\frac{m_{\pm i}^2}{m_\ell^2}, \frac{m_j^2}{m_\ell^2}\right),$$

$$\beta_{-1}^c(m_i, m_{\pm i}) = m_{\pm i}^4 - m_i^4,$$

$$\beta_0^c(m_i, m_{\pm i}) = m_{\pm i}^2 \log m_{\pm i}^2 - m_i^2 \log m_i^2,$$

$$\beta_1^c(m_\ell, m_i, m_{\pm i}) = 2m_{\pm i}^4 h\left(\frac{m_\ell^2}{m_{\pm i}^2}, 1\right) - 2m_i^4 h\left(\frac{m_\ell^2}{m_i^2}, 1\right) + m_\ell^2 m_{\pm i}^2 h\left(\frac{m_{\pm i}^2}{m_\ell^2}, \frac{m_{\pm i}^2}{m_\ell^2}\right) - m_\ell^2 m_i^2 h\left(\frac{m_i^2}{m_\ell^2}, \frac{m_i^2}{m_\ell^2}\right),$$

$$\beta_2^c(m_\ell, m_i, m_{\pm i}) = -m_{\pm i}^2 h\left(\frac{m_{\pm i}^2}{m_\ell^2}, \frac{m_{\pm i}^2}{m_\ell^2}\right) + m_i^2 h\left(\frac{m_i^2}{m_\ell^2}, \frac{m_i^2}{m_\ell^2}\right).$$

## A.2 One-node quiver

The quiver with just a single node reproduces the result of [35, 36]. Since the form factor is trivial, i.e.  $f(p^2) = 1$ , the non-zero coefficients are  $a_0 = b_0 = 1$ , see [103]. Hence, the mass function reads

$$\begin{aligned} \mathcal{E}_{\text{GMGM}} &= \sum_{\pm, i, j} (U_\pm^\dagger U_\mp)_{ij} (U_\mp^\dagger U_\pm)_{ji} \alpha_0^a(m_{\mp j}, m_{\pm i}) + \sum_{\pm, i, j} (U_\pm^\dagger)_{ij} (U_\pm)_{ji} \left( \alpha_0^b(m_j, m_{\pm i}) + \beta_0^b(m_j, m_{\pm i}) \right) \\ &\quad + \sum_{\pm, i} \beta_0^c(m_i, m_{\pm i}). \end{aligned} \quad (51)$$

## A.3 Two-nodes quiver

In this section we will calculate the example of the sfermion masses in two-nodes quiver-like models. In this model, there is only a single mass of the heavy vector bosons

$$\{m_\ell\} = m_v = \sqrt{2(g_A^2 + g_B^2)}v. \quad (52)$$

For the node  $A$ , the form factor is given by [104, 6, 105, 103]<sup>7</sup>

$$f_A(p^2) = \left( \frac{m_v^2}{p^2 - m_v^2} \right)^2, \quad (53)$$

which gives the coefficients

$$a_0 = 1, \quad a_1 = -1, \quad a_2 = -m_v^2, \quad b_{-1} = -\frac{2}{m_v^2}, \quad b_0 = 1, \quad b_1 = \frac{2}{m_v^2}, \quad b_2 = 1, \quad (54)$$

<sup>7</sup>For a  $5d$  model from which this form factor can be deconstructed, see also [106].

while for the node  $B$ , the form factor is

$$f_B(p^2) = \left( \frac{\lambda p^2 - m_v^2}{p^2 - m_v^2} \right)^2, \quad (55)$$

where  $\lambda = (g_A^2 + g_B^2)/g_A^2$  and the coefficients read [103]

$$\begin{aligned} a_0 &= 1, & a_1 &= -(1 - \lambda^2), & a_2 &= -(1 - \lambda)^2 m_v^2, \\ b_{-1} &= -\frac{2(1 - \lambda)}{m_v^2}, & b_0 &= 1, & b_1 &= \frac{2(1 - \lambda)}{m_v^2}, & b_2 &= (1 - \lambda)^2. \end{aligned} \quad (56)$$

The mass function is thus given by eq. (48) with the above coefficients.

### A.3.1 Large $m_v/M$ limit

From physical considerations, it is clear that in the limit of the Higgsing scale of the quiver,  $m_v$ , being much larger than the messenger scale,  $M$ , both of the above mass functions will reduce to that of the single node theory, eq. (51)

$$\lim_{\frac{m_v}{M} \rightarrow \infty} \mathcal{E}[f_A(p^2)] = \lim_{\frac{m_v}{M} \rightarrow \infty} \mathcal{E}[f_B(p^2)] = \mathcal{E}_{\text{GMGM}}. \quad (57)$$

However, in order to estimate how large  $m_v/M$  should be in order that the model is not at odds with meson mixings, the leading order in  $1/m_v^2$  correction is very useful and by expanding the functions (49-50), we obtain

$$\begin{aligned} \mathcal{E}[f_B(p^2)] &= \mathcal{E}_{\text{GMGM}} \\ &+ \sum_{\pm, i, j} (U_{\pm}^{\dagger} U_{\mp})_{ij} (U_{\mp}^{\dagger} U_{\pm})_{ji} \frac{(1 - \lambda^2) m_{\mp j}^2 m_{\pm i}^2}{2m_v^2} \left[ \log \left( \frac{m_v^2}{m_{\pm i}^2} \right) \log \left( \frac{m_v^2}{m_{\mp j}^2} \right) - \log \left( \frac{m_v^2}{m_{\mp j}^2} \right) - 1 + \frac{\pi^2}{3} \right] \\ &+ \sum_{\pm, i, j} (U_{\pm}^{\dagger})_{ij} (U_{\pm})_{ji} \frac{(1 - \lambda) m_j^2 m_{\pm i}^2}{m_v^2} \left[ - (2 + \lambda) \log^2 \left( \frac{m_v^2}{m_{\pm i}^2} \right) - \lambda \log^2 \left( \frac{m_v^2}{m_j^2} \right) + 2(1 + \lambda) \log \left( \frac{m_v^2}{m_j^2} \right) \right. \\ &\quad \left. + (1 + \lambda) \log^2 \left( \frac{m_{\pm i}^2}{m_j^2} \right) + 2(1 + \lambda) \left( 1 - \frac{\pi^2}{3} \right) \right] \\ &- \sum_{\pm, i, j} (U_{\pm}^{\dagger})_{ij} (U_{\pm})_{ji} \frac{2(1 - \lambda)(m_j^2 - m_{\pm i}^2)}{m_v^2} \left[ m_{\pm i}^2 \text{Li}_2 \left( 1 - \frac{m_j^2}{m_{\pm i}^2} \right) + m_j^2 \text{Li}_2 \left( 1 - \frac{m_{\pm i}^2}{m_j^2} \right) \right] \\ &+ \sum_{\pm, i} \left[ - \frac{(1 - \lambda)^2 m_{\pm i}^4}{2m_v^2} \log^2 \left( \frac{m_v^2}{m_{\pm i}^2} \right) + \frac{(2 + \lambda)(1 - \lambda) m_i^4}{m_v^2} \log^2 \left( \frac{m_v^2}{m_i^2} \right) - \frac{3(1 - \lambda^2) m_{\pm i}^4}{2m_v^2} \log \left( \frac{m_v^2}{m_{\pm i}^2} \right) \right. \\ &\quad \left. - \frac{m_{\pm i}^4}{2m_v^2} \left[ 3(1 - \lambda^2) + \frac{\pi^2}{3} (1 - \lambda)^2 \right] + \frac{(2 + \lambda)(1 - \lambda) m_i^4 \pi^2}{m_v^2} \frac{\pi^2}{3} \right] + \mathcal{O}(m_v^{-4}). \end{aligned} \quad (58)$$

The result for the node  $A$  is formally

$$\mathcal{E}[f_A(p^2)] = \mathcal{E}[f_B(p^2)]|_{\lambda=0}. \quad (59)$$

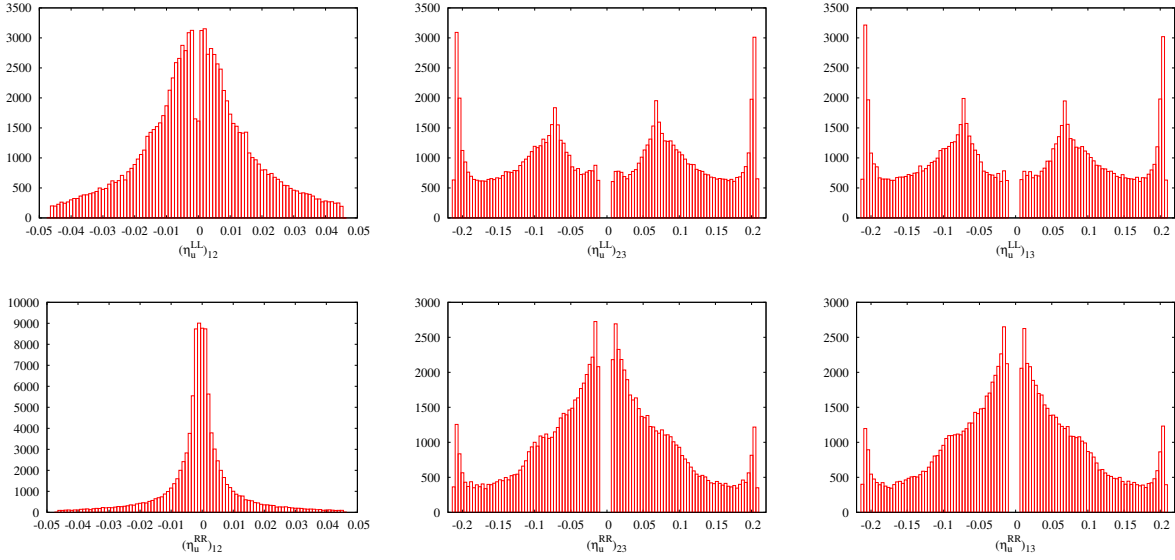


Figure 13: Monte Carlo analysis using the model flavor texture to obtain via the diagonalization matrices the elements  $(\eta_u^{LL,RR})_{ij}$ .

## B Monte Carlo analysis of diagonalization matrices

In this appendix we will use the flavor texture of eq. (2) with random coefficients in the range  $[0.1, 2]$  to generate realistic Yukawa matrices, i.e. reproducing the measured quark and lepton masses as well as the closest fit to the CKM matrix. Since there is remaining freedom in the basis of the Yukawas, we generate 100,000 random Yukawa matrices with coefficients in the above mentioned range  $[0.1, 2]$  multiplying the texture (2) – all giving physical Yukawas. Then we use the actual diagonalization matrices to calculate  $(\eta_{u,d}^{MM})_{ij} = (V_M^{u,d})_{i3}(V_M^{u,d\dagger})_{3j}$ , see eq. (24). In this analysis we have chosen  $\tan \beta = 20$ .

Using these data, we generate maximum and mean values for the  $\eta$ s, which are shown in tab. 4

## References

- [1] D. B. Kaplan, M. J. Savage and M. B. Wise, “A Perturbative calculation of the electromagnetic form-factors of the deuteron,” *Phys. Rev. C* **59**, 617 (1999) [nucl-th/9804032].
- [2] N. Arkani-Hamed, A. Gupta, D. E. Kaplan, N. Weiner and T. Zorawski, “Simply Unnatural Supersymmetry,” arXiv:1212.6971 [hep-ph].
- [3] C. Csaki, J. Erlich, C. Grojean and G. D. Kribs, “4-D constructions of supersymmetric extra dimensions and gaugino mediation,” *Phys. Rev. D* **65**, 015003 (2002) [hep-ph/0106044].
- [4] H. C. Cheng, D. E. Kaplan, M. Schmaltz and W. Skiba, “Deconstructing gaugino mediation,” *Phys. Lett. B* **515**, 395 (2001) [hep-ph/0106098].
- [5] N. Craig, D. Green and A. Katz, “(De)Constructing a Natural and Flavorful Supersymmetric Standard Model,” *JHEP* **1107**, 045 (2011) [arXiv:1103.3708 [hep-ph]].
- [6] R. Auzzi and A. Giveon, “The Sparticle spectrum in Minimal gaugino-Gauge Mediation,” *JHEP* **1010**, 088 (2010) [arXiv:1009.1714 [hep-ph]].

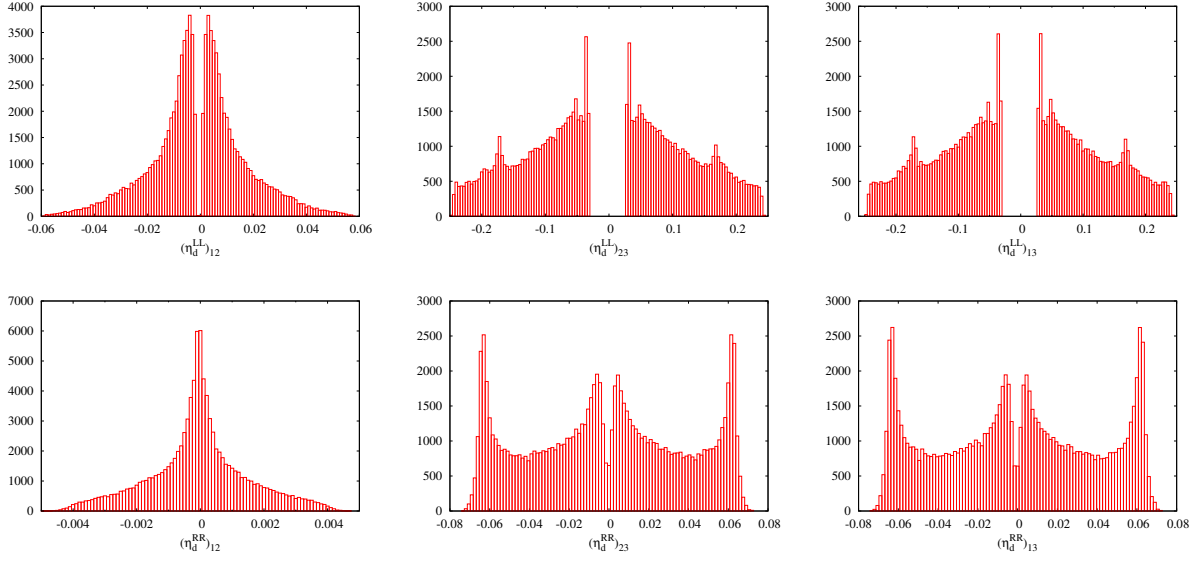


Figure 14: Monte Carlo analysis using the model flavor texture to obtain via the diagonalization matrices the elements  $(\eta_d^{LL,RR})_{ij}$ .

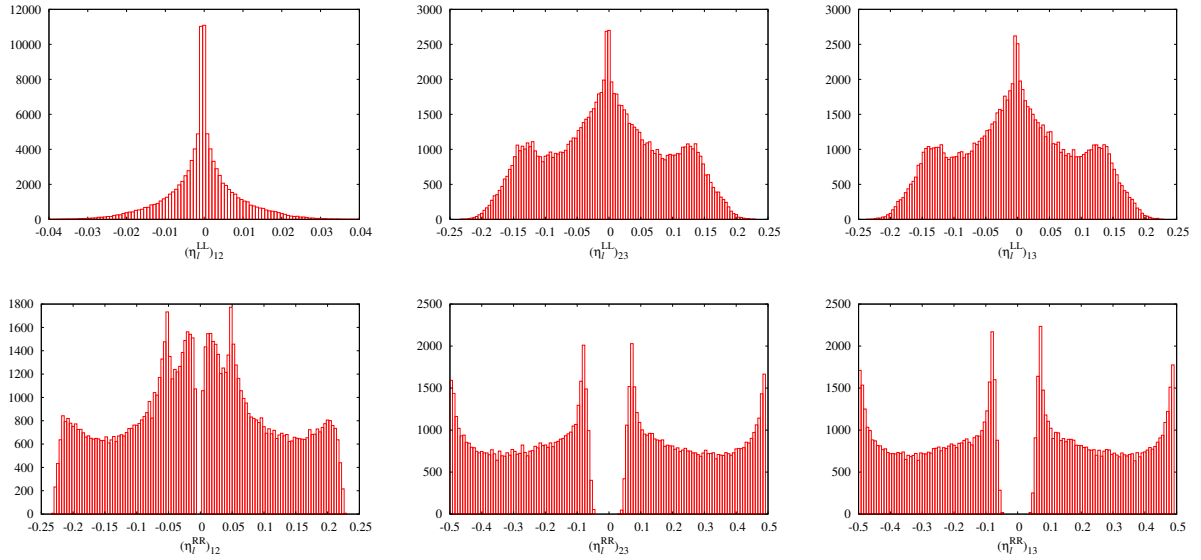


Figure 15: Monte Carlo analysis using the model flavor texture to obtain via the diagonalization matrices the elements  $(\eta_e^{LL})_{ij}, (\eta_e^{RR})_{ij}$ .

$X$	$\max(X)$	$\langle  X  \rangle$	$\sqrt{\langle X^2 \rangle}$
$(\eta_u^{LL})_{12}$	0.0463	0.0133	0.0172
$(\eta_u^{LL})_{23}$	0.2103	0.1106	0.1254
$(\eta_u^{LL})_{13}$	0.2101	0.1114	0.1261
$(\eta_u^{RR})_{12}$	0.0462	0.0072	0.0116
$(\eta_u^{RR})_{23}$	0.2102	0.0787	0.0974
$(\eta_u^{RR})_{13}$	0.2103	0.0800	0.0986
$(\eta_d^{LL})_{12}$	0.0584	0.0134	0.0175
$(\eta_d^{LL})_{23}$	0.2452	0.1116	0.1265
$(\eta_d^{LL})_{13}$	0.2455	0.1122	0.1273
$(\eta_d^{RR})_{12}$	0.0049	0.0011	0.0015
$(\eta_d^{RR})_{23}$	0.0729	0.0334	0.0397
$(\eta_d^{RR})_{13}$	0.0734	0.0340	0.0402
$(\eta_\ell^{LL})_{12}$	0.0530	0.0060	0.0088
$(\eta_\ell^{LL})_{23}$	0.2314	0.0743	0.0914
$(\eta_\ell^{LL})_{13}$	0.2327	0.0750	0.0920
$(\eta_e^{RR})_{12}$	0.2291	0.0969	0.1169
$(\eta_e^{RR})_{23}$	0.4954	0.2645	0.2994
$(\eta_e^{RR})_{13}$	0.4955	0.2660	0.3009

Table 4: Maximum, average and second moment average of the  $\eta$  elements, calculated by the Monte Carlo method.

- [7] R. Auzzi and A. Giveon, “Superpartner spectrum of minimal gaugino-gauge mediation,” JHEP **1101**, 003 (2011) [arXiv:1011.1664 [hep-ph]].
- [8] R. Auzzi, A. Giveon, S. B. Gudnason and T. Shacham, “On the Spectrum of Direct Gaugino Mediation,” JHEP **1109**, 108 (2011) [arXiv:1107.1414 [hep-ph]].
- [9] R. Auzzi, A. Giveon and S. B. Gudnason, “Flavor of quiver-like realizations of effective supersymmetry,” JHEP **1202**, 069 (2012) [arXiv:1112.6261 [hep-ph]].
- [10] R. Auzzi, A. Giveon, S. B. Gudnason and T. Shacham, “A Light Stop with Flavor in Natural SUSY,” JHEP **1301**, 169 (2013) [arXiv:1208.6263 [hep-ph]].
- [11] N. Arkani-Hamed and S. Dimopoulos, “Supersymmetric unification without low energy supersymmetry and signatures for fine-tuning at the LHC,” JHEP **0506**, 073 (2005) [hep-th/0405159].
- [12] G. F. Giudice and A. Romanino, “Split supersymmetry,” Nucl. Phys. B **699**, 65 (2004) [Erratum-ibid. B **706**, 65 (2005)] [hep-ph/0406088].
- [13] N. Arkani-Hamed, S. Dimopoulos, G. F. Giudice and A. Romanino, “Aspects of split supersymmetry,” Nucl. Phys. B **709**, 3 (2005) [hep-ph/0409232].
- [14] D. Green, A. Katz and Z. Komargodski, “Direct Gaugino Mediation,” Phys. Rev. Lett. **106**, 061801 (2011) [arXiv:1008.2215 [hep-th]].



- [15] G. Aad *et al.* [ATLAS Collaboration], “Observation of a new particle in the search for the Standard Model Higgs boson with the ATLAS detector at the LHC,” *Phys. Lett. B* **716**, 1 (2012) [arXiv:1207.7214 [hep-ex]].
- [16] S. Chatrchyan *et al.* [CMS Collaboration], “Observation of a new boson at a mass of 125 GeV with the CMS experiment at the LHC,” *Phys. Lett. B* **716**, 30 (2012) [arXiv:1207.7235 [hep-ex]].
- [17] S. P. Martin, “A Supersymmetry primer,” In \*Kane, G.L. (ed.): Perspectives on supersymmetry II\* 1-153 [hep-ph/9709356].
- [18] T. Gherghetta, G. F. Giudice and A. Riotto, “Nucleosynthesis bounds in gauge mediated supersymmetry breaking theories,” *Phys. Lett. B* **446**, 28 (1999) [hep-ph/9808401].
- [19] G. F. Giudice and R. Rattazzi, “Theories with gauge mediated supersymmetry breaking,” *Phys. Rept.* **322**, 419 (1999) [hep-ph/9801271].
- [20] Z. Komargodski and D. Shih, “Notes on SUSY and R-Symmetry Breaking in Wess-Zumino Models,” *JHEP* **0904**, 093 (2009) [arXiv:0902.0030 [hep-th]].
- [21] **ATLAS** Collaboration, “Search for Supersymmetry in Events with Large Missing Transverse Momentum, Jets, and at Least One Tau Lepton in 21  $fb^{-1}$  of  $\sqrt{s} = 8$  TeV Proton-Proton Collision Data with the ATLAS Detector,” ATLAS-CONF-2013-026.
- [22] A. Giveon, A. Katz and Z. Komargodski, “Uplifted Metastable Vacua and Gauge Mediation in SQCD,” *JHEP* **0907**, 099 (2009) [arXiv:0905.3387 [hep-th]].
- [23] R. Auzzi, S. Elitzur and A. Giveon, “On Uplifted SUSY-Breaking Vacua and Direct Mediation in Generalized SQCD,” *JHEP* **1003**, 094 (2010) [arXiv:1001.1234 [hep-th]].
- [24] M. Baryakhtar, E. Hardy and J. March-Russell, “Axion Mediation,” arXiv:1301.0829 [hep-ph].
- [25] B. C. Allanach, “SOFTSUSY: a program for calculating supersymmetric spectra,” *Comput. Phys. Commun.* **143**, 305 (2002) [hep-ph/0104145].
- [26] **ATLAS** Collaboration, “Search for direct production of charginos and neutralinos in events with three leptons and missing transverse momentum in 21  $fb^{-1}$  of pp collisions at  $\sqrt{s} = 8$  TeV with the ATLAS detector,” ATLAS-CONF-2013-035
- [27] P. Meade, M. Reece and D. Shih, “Prompt Decays of General Neutralino NLSPs at the Tevatron,” *JHEP* **1005**, 105 (2010) [arXiv:0911.4130 [hep-ph]].
- [28] **ATLAS** Collaboration, “Combined measurements of the mass and signal strength of the Higgs-like boson with the ATLAS detector using up to 24 $fb^{-1}$  of proton-proton collision data,” ATLAS-CONF-2013-014.
- [29] P. P. Giardino, K. Kannike, I. Masina, M. Raidal and A. Strumia, “The universal Higgs fit,” arXiv:1303.3570 [hep-ph].
- [30] R. Barbieri and G. F. Giudice, “Upper Bounds on Supersymmetric Particle Masses,” *Nucl. Phys. B* **306**, 63 (1988).
- [31] A. Djouadi, M. M. Muhlleitner and M. Spira, “Decays of supersymmetric particles: The Program SUSY-HIT (SUSpect-SdecaY-Hdecay-InTerface),” *Acta Phys. Polon. B* **38**, 635 (2007) [hep-ph/0609292].

- [32] A. Arvanitaki, N. Craig, S. Dimopoulos and G. Villadoro, “Mini-Split,” JHEP **1302**, 126 (2013) [arXiv:1210.0555 [hep-ph]].
- [33] K. Howe and P. Saraswat, “Excess Higgs Production in Neutralino Decays,” JHEP **1210**, 065 (2012) [arXiv:1208.1542 [hep-ph]].
- [34] **ATLAS** Collaboration, “Search for direct-slepton and direct-chargino production in final states with two opposite-sign leptons, missing transverse momentum and no jets in 20/fb of pp collisions at  $\sqrt{s} = 8$  TeV with the ATLAS detector,” ATLAS-CONF-2013-049.
- [35] D. Marques, “Generalized messenger sector for gauge mediation of supersymmetry breaking and the soft spectrum,” JHEP **0903**, 038 (2009) [arXiv:0901.1326 [hep-ph]].
- [36] T. T. Dumitrescu, Z. Komargodski, N. Seiberg and D. Shih, “General Messenger Gauge Mediation,” JHEP **1005**, 096 (2010) [arXiv:1003.2661 [hep-ph]].
- [37] J. Beringer *et al.* [Particle Data Group Collaboration], “Review of Particle Physics (RPP),” Phys. Rev. D **86**, 010001 (2012).
- [38] O. Gedalia and G. Perez, “TASI 2009 Lectures - Flavor Physics,” arXiv:1005.3106 [hep-ph].
- [39] S. Jager, “Supersymmetry beyond minimal flavour violation,” Eur. Phys. J. C **59**, 497 (2009) [arXiv:0808.2044 [hep-ph]].
- [40] L. J. Hall, V. A. Kostelecky and S. Raby, “New Flavor Violations in Supergravity Models,” Nucl. Phys. B **267**, 415 (1986).
- [41] G. F. Giudice, M. Nardecchia and A. Romanino, “Hierarchical Soft Terms and Flavor Physics,” Nucl. Phys. B **813**, 156 (2009) [arXiv:0812.3610 [hep-ph]].
- [42] S. Dimopoulos and G. F. Giudice, “Naturalness constraints in supersymmetric theories with nonuniversal soft terms,” Phys. Lett. B **357**, 573 (1995) [hep-ph/9507282].
- [43] A. G. Cohen, D. B. Kaplan and A. E. Nelson, “The More minimal supersymmetric standard model,” Phys. Lett. B **388**, 588 (1996) [hep-ph/9607394].
- [44] R. Barbieri, E. Bertuzzo, M. Farina, P. Lodone and D. Pappadopulo, “A Non Standard Supersymmetric Spectrum,” JHEP **1008**, 024 (2010) [arXiv:1004.2256 [hep-ph]].
- [45] R. Barbieri, G. Isidori, J. Jones-Perez, P. Lodone and D. M. Straub, “U(2) and Minimal Flavour Violation in Supersymmetry,” Eur. Phys. J. C **71**, 1725 (2011) [arXiv:1105.2296 [hep-ph]].
- [46] C. Brust, A. Katz, S. Lawrence and R. Sundrum, “SUSY, the Third Generation and the LHC,” JHEP **1203**, 103 (2012) [arXiv:1110.6670 [hep-ph]].
- [47] M. Papucci, J. T. Ruderman and A. Weiler, “Natural SUSY Endures,” JHEP **1209**, 035 (2012) [arXiv:1110.6926 [hep-ph]].
- [48] J. S. Hagelin, S. Kelley and T. Tanaka, “Supersymmetric flavor changing neutral currents: Exact amplitudes and phenomenological analysis,” Nucl. Phys. B **415**, 293 (1994).
- [49] F. Gabbiani, E. Gabrielli, A. Masiero and L. Silvestrini, “A Complete analysis of FCNC and CP constraints in general SUSY extensions of the standard model,” Nucl. Phys. B **477**, 321 (1996) [hep-ph/9604387].

- [50] W. Altmannshofer, A. J. Buras, S. Gori, P. Paradisi and D. M. Straub, “Anatomy and Phenomenology of FCNC and CPV Effects in SUSY Theories,” Nucl. Phys. B **830**, 17 (2010) [arXiv:0909.1333 [hep-ph]].
- [51] J. A. Bagger, K. T. Matchev and R. -J. Zhang, “QCD corrections to flavor changing neutral currents in the supersymmetric standard model,” Phys. Lett. B **412**, 77 (1997) [hep-ph/9707225].
- [52] M. Ciuchini, V. Lubicz, L. Conti, A. Vladikas, A. Donini, E. Franco, G. Martinelli and I. Scimemi *et al.*, “Delta M(K) and epsilon(K) in SUSY at the next-to-leading order,” JHEP **9810**, 008 (1998) [hep-ph/9808328].
- [53] R. Contino and I. Scimemi, “The Supersymmetric flavor problem for heavy first two generation scalars at next-to-leading order,” Eur. Phys. J. C **10**, 347 (1999) [hep-ph/9809437].
- [54] P. A. Boyle *et al.* [RBC and UKQCD Collaborations], “Neutral kaon mixing beyond the standard model with  $n_f = 2 + 1$  chiral fermions,” Phys. Rev. D **86**, 054028 (2012) [arXiv:1206.5737 [hep-lat]].
- [55] V. Bertone *et al.* [for the ETM Collaboration], “Kaon Mixing Beyond the SM from  $N_f=2$  tmQCD and model independent constraints from the UTA,” JHEP **1303**, 089 (2013) [arXiv:1207.1287 [hep-lat]].
- [56] M. Misiak, S. Pokorski and J. Rosiek, “Supersymmetry and FCNC effects,” Adv. Ser. Direct. High Energy Phys. **15**, 795 (1998) [hep-ph/9703442].
- [57] S. P. Martin and M. T. Vaughn, “Two loop renormalization group equations for soft supersymmetry breaking couplings,” Phys. Rev. D **50**, 2282 (1994) [Erratum-ibid. D **78**, 039903 (2008)] [hep-ph/9311340].
- [58] Y. Amhis *et al.* [Heavy Flavor Averaging Group Collaboration], “Averages of B-Hadron, C-Hadron, and tau-lepton properties as of early 2012,” arXiv:1207.1158 [hep-ex].
- [59] J. Adam *et al.* [MEG Collaboration], “New constraint on the existence of the  $\mu^+ \rightarrow e^+\gamma$  decay,” arXiv:1303.0754 [hep-ex].
- [60] J. J. Hudson, D. M. Kara, I. J. Smallman, B. E. Sauer, M. R. Tarbutt and E. A. Hinds, “Improved measurement of the shape of the electron,” Nature **473**, 493 (2011).
- [61] C. A. Baker, D. D. Doyle, P. Geltenbort, K. Green, M. G. D. van der Grinten, P. G. Harris, P. Iaydjiev and S. N. Ivanov *et al.*, “An Improved experimental limit on the electric dipole moment of the neutron,” Phys. Rev. Lett. **97**, 131801 (2006) [hep-ex/0602020].
- [62] D. Becirevic, M. Ciuchini, E. Franco, V. Gimenez, G. Martinelli, A. Masiero, M. Papinutto and J. Reyes *et al.*, “ $B_d - \bar{B}_d$  mixing and the  $B_d \rightarrow J/\psi K_s$  asymmetry in general SUSY models,” Nucl. Phys. B **634**, 105 (2002) [hep-ph/0112303].
- [63] M. Bona *et al.* [UTfit Collaboration], “Model-independent constraints on  $\Delta F=2$  operators and the scale of new physics,” JHEP **0803**, 049 (2008) [arXiv:0707.0636 [hep-ph]].
- [64] P. Paradisi, “Constraints on SUSY lepton flavor violation by rare processes,” JHEP **0510**, 006 (2005) [hep-ph/0505046].
- [65] F. Gabbiani and A. Masiero, “FCNC in Generalized Supersymmetric Theories,” Nucl. Phys. B **322**, 235 (1989).

- [66] A. M. Baldini, F. Cei, C. Cerri, S. Dussoni, L. Galli, M. Grassi, D. Nicolo and F. Raffaelli *et al.*, “MEG Upgrade Proposal,” arXiv:1301.7225 [physics.ins-det].
- [67] T. Moroi and M. Nagai, “Probing Supersymmetric Model with Heavy Sfermions Using Leptonic Flavor and CP Violations,” Phys. Lett. B **723**, 107 (2013) [arXiv:1303.0668 [hep-ph]].
- [68] T. Moroi, M. Nagai and T. T. Yanagida, “Lepton Flavor Violations in High-Scale SUSY with Right-Handed Neutrinos,” arXiv:1305.7357 [hep-ph].
- [69] T. Hermann, M. Misiak and M. Steinhauser, “ $\bar{B} \rightarrow X_s \gamma$  in the Two Higgs Doublet Model up to Next-to-Next-to-Leading Order in QCD,” JHEP **1211**, 036 (2012) [arXiv:1208.2788 [hep-ph]].
- [70] J. Hisano, M. Nagai and P. Paradisi, “New Two-loop Contributions to Hadronic EDMs in the MSSM,” Phys. Lett. B **642**, 510 (2006) [hep-ph/0606322].
- [71] M. Pospelov and A. Ritz, “Neutron EDM from electric and chromoelectric dipole moments of quarks,” Phys. Rev. D **63**, 073015 (2001) [hep-ph/0010037].
- [72] J. Hisano, M. Nagai and P. Paradisi, “Flavor effects on the electric dipole moments in supersymmetric theories: A beyond leading order analysis,” Phys. Rev. D **80**, 095014 (2009) [arXiv:0812.4283 [hep-ph]].
- [73] A. C. Vutha, W. C. Campbell, Y. V. Gurevich, N. R. Hutzler, M. Parsons, D. Patterson, E. Petrik and B. Spaun *et al.*, “Search for the electric dipole moment of the electron with thorium monoxide,” J. Phys. B **43**, 074007 (2010) [arXiv:0908.2412 [physics.atom-ph]].
- [74] B. L. Roberts, “Status of the Fermilab Muon ( $g - 2$ ) Experiment,” Chin. Phys. C **34**, 741 (2010) [arXiv:1001.2898 [hep-ex]].
- [75] T. Moroi, “The Muon anomalous magnetic dipole moment in the minimal supersymmetric standard model,” Phys. Rev. D **53**, 6565 (1996) [Erratum-ibid. D **56**, 4424 (1997)] [hep-ph/9512396].
- [76] M. Endo, K. Hamaguchi, S. Iwamoto and T. Yoshinaga, “Muon  $g-2$  vs LHC in Supersymmetric Models,” arXiv:1303.4256 [hep-ph].
- [77] M. Bolz, A. Brandenburg and W. Buchmuller, “Thermal production of gravitinos,” Nucl. Phys. B **606**, 518 (2001) [Erratum-ibid. B **790**, 336 (2008)] [hep-ph/0012052].
- [78] P. A. R. Ade *et al.* [Planck Collaboration], “Planck 2013 results. XVI. Cosmological parameters,” arXiv:1303.5076 [astro-ph.CO].
- [79] M. Fukugita and T. Yanagida, “Baryogenesis Without Grand Unification,” Phys. Lett. B **174**, 45 (1986).
- [80] S. Davidson and A. Ibarra, “A Lower bound on the right-handed neutrino mass from leptogenesis,” Phys. Lett. B **535**, 25 (2002) [hep-ph/0202239].
- [81] V. S. Rychkov and A. Strumia, “Thermal production of gravitinos,” Phys. Rev. D **75**, 075011 (2007) [hep-ph/0701104].
- [82] T. Moroi, H. Murayama and M. Yamaguchi, “Cosmological constraints on the light stable gravitino,” Phys. Lett. B **303**, 289 (1993).

- [83] M. Kawasaki, K. Kohri, T. Moroi and A. Yotsuyanagi, “Big-Bang Nucleosynthesis and Gravitino,” *Phys. Rev. D* **78**, 065011 (2008) [arXiv:0804.3745 [hep-ph]].
- [84] J. R. Ellis, J. E. Kim and D. V. Nanopoulos, “Cosmological Gravitino Regeneration and Decay,” *Phys. Lett. B* **145**, 181 (1984).
- [85] W. Hu and J. Silk, “Thermalization constraints and spectral distortions for massive unstable relic particles,” *Phys. Rev. Lett.* **70**, 2661 (1993).
- [86] D. J. Fixsen, E. S. Cheng, J. M. Gales, J. C. Mather, R. A. Shafer and E. L. Wright, “The Cosmic Microwave Background spectrum from the full COBE FIRAS data set,” *Astrophys. J.* **473**, 576 (1996) [astro-ph/9605054].
- [87] J. L. Feng, A. Rajaraman and F. Takayama, “SuperWIMP dark matter signals from the early universe,” *Phys. Rev. D* **68**, 063504 (2003) [hep-ph/0306024].
- [88] H. Yuksel and M. D. Kistler, “Circumscribing late dark matter decays model independently,” *Phys. Rev. D* **78**, 023502 (2008) [arXiv:0711.2906 [astro-ph]].
- [89] J. L. Feng, S. Su and F. Takayama, “Supergravity with a gravitino LSP,” *Phys. Rev. D* **70**, 075019 (2004) [hep-ph/0404231].
- [90] J. R. Ellis, K. A. Olive, Y. Santoso and V. C. Spanos, “Gravitino dark matter in the CMSSM,” *Phys. Lett. B* **588**, 7 (2004) [hep-ph/0312262].
- [91] L. Boubekur, K. Y. Choi, R. Ruiz de Austri and O. Vives, “The degenerate gravitino scenario,” *JCAP* **1004**, 005 (2010) [arXiv:1002.0340 [hep-ph]].
- [92] A. Boyarsky, J. Lesgourgues, O. Ruchayskiy and M. Viel, “Lyman-alpha constraints on warm and on warm-plus-cold dark matter models,” *JCAP* **0905**, 012 (2009) [arXiv:0812.0010 [astro-ph]].
- [93] R. S. de Souza, A. Mesinger, A. Ferrara, Z. Haiman, R. Perna and N. Yoshida, “Constraints on Warm Dark Matter models from high-redshift long gamma-ray bursts,” arXiv:1303.5060 [astro-ph.CO].
- [94] A. V. Maccio, S. Paduroiu, D. Anderhalden, A. Schneider and B. Moore, “Cores in warm dark matter haloes: a Catch 22 problem,” arXiv:1202.1282 [astro-ph.CO].
- [95] X. Kang, A. V. Maccio and A. A. Dutton, “The effect of Warm Dark Matter on galaxy properties: constraints from the stellar mass function and the Tully-Fisher relation,” *Astrophys. J.* **767**, 22 (2013) [arXiv:1208.0008 [astro-ph.CO]].
- [96] R. E. Angulo, O. Hahn and T. Abel, “The Warm DM halo mass function below the cut-off scale,” arXiv:1304.2406 [astro-ph.CO].
- [97] H. J. de Vega and N. G. Sanchez, arXiv:1304.0759 [astro-ph.CO].
- [98] N. Menci, F. Fiore and A. Lamastra, “The Evolution of Active Galactic Nuclei in Warm Dark Matter Cosmology,” *Astrophys. J.* **766**, 110 (2013) [arXiv:1302.2000 [astro-ph.CO]].
- [99] D. Shih, “Pseudomoduli Dark Matter,” *JHEP* **0909**, 046 (2009) [arXiv:0906.3346 [hep-ph]].
- [100] B. Keren-Zur, L. Mazzucato and Y. Oz, “Dark Matter and Pseudo-flat Directions in Weakly Coupled SUSY Breaking Sectors,” *JHEP* **0909**, 041 (2009) [arXiv:0906.5586 [hep-ph]].

- [101] S. Dimopoulos, G. F. Giudice and A. Pomarol, “Dark matter in theories of gauge mediated supersymmetry breaking,” *Phys. Lett. B* **389**, 37 (1996) [hep-ph/9607225].
- [102] P. Gambino, G. F. Giudice and P. Slavich, “Gluino decays in split supersymmetry,” *Nucl. Phys. B* **726**, 35 (2005) [hep-ph/0506214].
- [103] R. Auzzi, A. Gaiotto and S. B. Gukov, “Mediation of Supersymmetry Breaking in Quivers,” *JHEP* **1112**, 016 (2011) [arXiv:1110.1453 [hep-ph]].
- [104] M. McGarrie, “General Gauge Mediation and Deconstruction,” *JHEP* **1011**, 152 (2010) [arXiv:1009.0012 [hep-ph]].
- [105] M. Sudano, “General Gaugino Mediation,” arXiv:1009.2086 [hep-ph].
- [106] M. McGarrie and R. Russo, “General Gauge Mediation in 5D,” *Phys. Rev. D* **82**, 035001 (2010) [arXiv:1004.3305 [hep-ph]].